Title
Changing the Drug Exposure of Small Molecule Tyrosine Kinase Inhibitors

Author
Yago, Marc Anthony Ramos

Publication Date
2015

Peer reviewed|Thesis/dissertation

Changing the Drug Exposure of Small Molecule
Tyrosine Kinase Inhibitors

by

Marc Anthony R. Yago

DISSERTATION

Submitted in partial satisfaction of the requirements for the degree of

DOCTOR OF PHILOSOPHY

in

Pharmaceutical Sciences and Pharmacogenomics

in the

GRADUATE DIVISION

of the

UNIVERSITY OF CALIFORNIA, SAN FRANCISCO

Dedicated to

my mom and dad, Marissa and Celso,

my little brother, Scotty,

and all of my family and friends,

whose unconditional love, support, and unwavering faith

has always been my source of inspiration.

ACKNOWLEDGEMENTS

The text of Chapter 2 is a modified version of the material as it appears in *Molecular Pharmaceutics*. MRY participated in the design and execution of the study, performed the analyses, and wrote the manuscript. AF participated in the design and execution of the study, and assisted with data analysis and manuscript preparation. GSS, LAF, NRB, MJD, and JAW assisted with study design and manuscript preparation. LZB assisted with study design, data analysis and manuscript preparation.

The text of Chapter 3 is a modified version of the material as it appears in *The AAPS Journal*. MRY participated in the design and execution of the study, performed all analyses, and wrote the manuscript. AF, LZB, GSS, LAF, NRB and JAW assisted with study design, data analysis and manuscript preparation. LS and JYJ assisted with early study design. XD, BD, and MJD provided resources for the bioanalysis of dasatinib and rabeprazole.

Completing a doctoral degree is by no means an easy task, and I have been so fortunate to have had the guidance and support of so many individuals along the way.

I would first like to thank my advisor and mentor, Dr. Leslie Benet, for giving me the opportunity to work in his laboratory and for all of his support and encouragement throughout my graduate school career. Working with Les has been particularly enlightening for me as a student of the drug developmental sciences as he is extremely knowledgeable of a wide breadth of subjects in the pharmaceutical industry. He has an innate ability to explain things with such clarity and always made me feel that I can accomplish anything. His mentorship and enthusiasm for science is contagious and evident in all of his students, and I hope one day to be the positive influence on a young scientific mind in the same way that Les was for me.

I would also like to thank Frances Peterson not only for being our liaison to Les, but for also being the "auntie" of the lab. From appointments, to submitting manuscripts, and everything else in between, Frances has always been that person who helped make things happen. Our conversations about food, culture, music and faith in between all of the science were a much welcomed break and I will always cherish them.

Here at UCSF, faculty members are an integral part of the scientific and personal growth of young scientists. Thus I am truly thankful for Drs. Sara Kenkare-Mitra and Neil Shah for their guidance on my thesis project and the construction of this dissertation. I would also like to thank Drs. Matt Jacobson, Neal Benowitz, Michael Fischbach, and Neil Shah for serving on my qualifying exam committee and providing me with insightful comments and critiques during my exam.

My particular project gave me the opportunity to gain clinical experience by designing and executing clinical studies with healthy volunteers. For that, I am extremely grateful for the

mentorship of Drs. Lynda Frassetto and Adam Frymoyer, who have both guided me through my interactions with our healthy volunteers and the UCSF institutional review board. Without them, I would still be lost amongst the countless forms necessary to screen a single subject. I would also like to thank Dr. Joseph Ware (Genentech, Inc.) and Gillian Smelick (formerly Genentech, Inc.) for their valuable insights throughout our collaboration, and for making my internship in the Clinical Pharmacology department at Genentech an exciting and eye-opening experience.

I am also thankful for all of the Benet Lab members that I have been fortunate enough to work with over the years. From the post-group meeting discussions to the lunch outings and numerous quals practices, my experiences in the lab would not have been the same without them. I would like to especially thank Dr. Hideaki Okochi for teaching me everything I needed to know about cells and cell culture as I would not have finished Chapter 4 without his assistance. I also extend my thanks to Alan Wolfe for making sure that the lab is always running smoothly, especially regarding protocols, supplies, and maintenance.

I also express my gratitude for my fellow PSPG colleagues and classmates, especially Drs. Howard Horng (Grandpa) and Kari Morrissey (Mom). Howard and Kari have been fantastic mentors throughout graduate school and taught me what it means to really put your heart into your research. Howard, thank you for bestowing upon me all of the LC-MS/MS experience I needed and for showing me that you can indeed work hard and play hard. Kari, you were always someone I could turn to for advice on life, love, and family, and I will be forever thankful for all of our heart-to-heart conversations. I am also extremely grateful to have worked with Dr. Connie Remsberg and Chelsea Hosey, who were my “sisters” in the lab and did well to keep me grounded through all of my frustrations.

A special thanks to Drs. Tiffany Chung, Xue Vee Yang, Lena Yoo, and Nghi Ha for helping me balance work with movies, food, and Lake Tahoe. I wish you the best in all of your future endeavors, wherever they may take you.

I could not have finished this degree without the love and support of all of my family members, whose endless sacrifices and belief in me have allowed me to accomplish all of my goals thus far. Mom, thank you for pushing me as a child to understand the value of a good education and for teaching me to put the needs of others before my own. Dad, you have literally given me a second chance at life and in doing so, have shown me what it means to take care of your own. I cannot begin to express how thankful I am to be your son. Scotty, I cannot thank you enough for being my partner-in-crime and my little brother. You make coming home so much fun, and I hope one day you will be able to accomplish all of your endeavors as well.

Finally, I would like to thank my love, Dr. Vanessa Shih, for her unending love and support throughout graduate school. Vanessa, thank you for being my cheerleader, for telling me that "it'll be okay," and for putting up with me while I get up in the middle of the night to switch my samples on the LC-MS/MS. You mean the world to me and I cannot wait to see what the future has in store for us. I love you "∞ x ∞."

ABSTRACT

CHANGING THE DRUG EXPOSURE OF SMALL MOLECULE TYROSINE KINASE INHIBITORS

MARC ANTHONY R. YAGO

Tyrosine kinase inhibitors (TKIs) are a class of targeted oncologic therapies designed to inhibit the phosphorylation of tyrosine residues on cellular proteins typically involved in various cell signaling pathways. Particularly for small molecule TKIs, these drugs compete with ATP for binding in the intracellular catalytic domains of tyrosine kinases that possess specific mutations or that are overexpressed in cancer cells, which results in a constitutively active kinase. As the efficacy of TKIs is largely dependent on sufficient drug exposure in the body, pharmacokinetic interactions that alter systemic concentrations of TKIs can either reduce drug exposures to subtherapeutic levels, or raise drug exposures past toxicity limits.

Many of the small molecule TKIs are weakly basic drugs whose solubility decreases at an elevated pH. It is for this reason that TKIs are often advised in their labeling not to be co-administered with acid-reducing agents, such as proton pump inhibitors or H_2-receptor antagonists, as prolonged usage of acid-reducing agents can result in an elevated fasting gastric pH, also known as hypochlorhydria. Additionally, many TKIs are extensively metabolized in the liver by cytochrome P450 enzymes. Therefore drug-drug interactions that impact mechanisms of hepatic uptake (i.e. uptake transporters) will result in a reduced hepatic clearance and an increased risk of drug toxicity.

Therefore we hypothesize that the drug disposition of small molecule TKIs can be affected by gastric pH and hepatic uptake transporters, which are viable targets for drug-drug interactions that may cause significant changes in drug exposure. The research presented herein evaluates the impact of gastric pH on the pharmacokinetics of dasatinib, a TKI with pH-dependent solubility, in healthy volunteers with rabeprazole (a proton-pump inhibitor)-induced hypochlorhydria, and proposes the use of betaine hydrochloride as a potential mitigation strategy. The research presented also utilizes the Biopharmaceutics Drug Disposition Classification System to predict mechanisms of hepatic uptake and the potential effects of hepatic uptake transporters on liver disposition of three selected TKIs: dasatinib, bosutinib, and vandetanib. Collectively, these studies aim to highlight potential areas of drug development for TKIs that may translate to more effective treatment of oncology patients.

TABLE OF CONTENTS

LIST OF TABLES

LIST OF FIGURES

CHAPTER 1. CHALLENGES IN THE DEVELOPMENT AND USE OF TYROSINE KINASE INHIBITORS

TYROSINE KINASES

Over 500 protein kinases have been identified in the human kinome, of which 90 belong to the tyrosine- or tyrosine-like kinase families (1). These kinases are responsible for the phosphorylation of various cellular proteins via the transfer of the gamma phosphate group of adenosine-triphosphate (ATP) to a hydroxyl group (–OH) located on free tyrosine, serine, or threonine residues (**Figure 1.1**). These phosphorylation events then cause conformational changes in the protein, leading to activation or inactivation of signal transduction cascades (2).

The kinases in the tyrosine- and tyrosine-like families (henceforth collectively referred to as the tyrosine kinase family) are categorized into two groups: receptor tyrosine kinases and nonreceptor tyrosine kinases (**Figure 1.2**). Receptor tyrosine kinases (RTKs) have three general domains that span extra- and intracellular environments: an extracellular ligand-binding domain, a transmembrane domain, and an intracellular catalytic domain. The extracellular domain is responsible for the binding of soluble ligands and acts as a receptor in response to the extracellular environment (3), thus giving RTKs their name. The transmembrane domain of RTKs usually consists of α-helices that act to facilitate and stabilize dimerization upon kinase activation (4). Last, the intracellular catalytic domain protrudes into the cytoplasm of cells and contains sites for auto-phosphorylation and the phosphorylation of substrates (3).

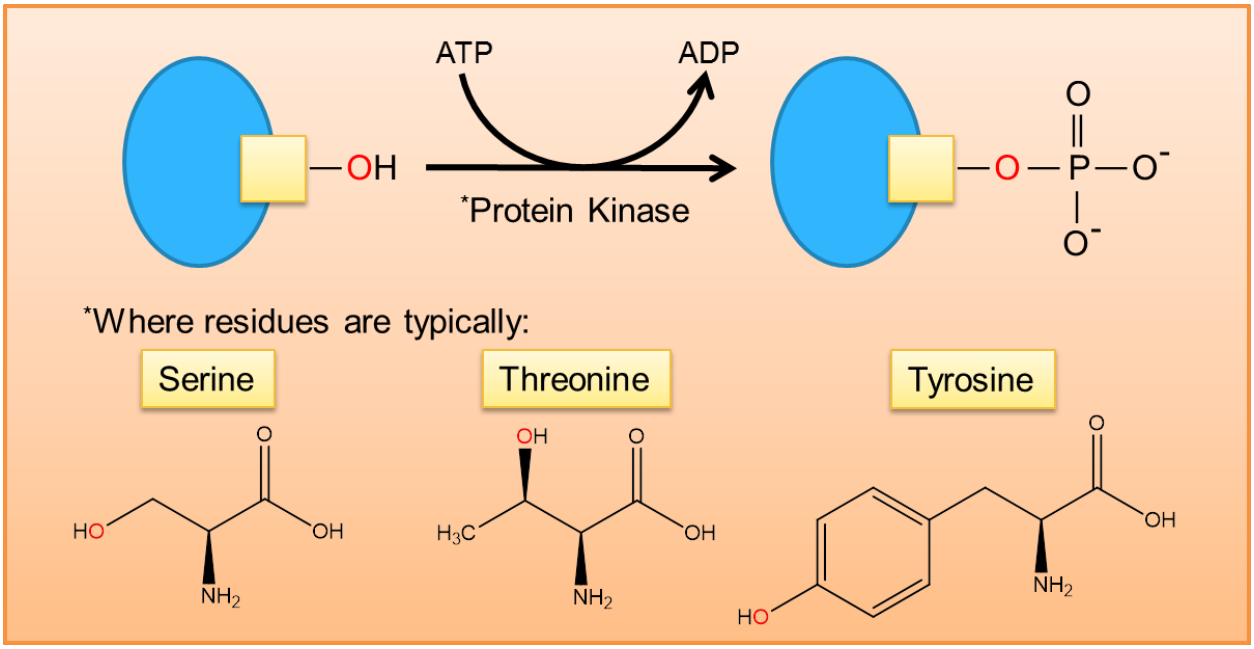

Figure 1.1 Phosphorylation of proteins via tyrosine- or tyrosine-like kinases. Tyrosine kinases catalyze the transfer of gamma phosphate groups of ATP specifically to free tyrosine residues, whereas tyrosine-like kinases will phosphorylate free serine or threonine residues on proteins.

Activation of RTKs is dependent on ligand-binding events that occur at the extracellular ligand-binding domain. For example, the epidermal growth factor receptor (EGFR) requires binding the ligands EGF or transforming growth factor-α (TGF-α) to initiate kinase activation (5). Upon binding of the ligand, EGFR then dimerizes, forming homo- or heterodimers with other EGFRs, which fosters intermolecular interactions and transphosphorylation in the intracellular catalytic domains between monomers. The transphosphorylation events then reposition the activation loop of the catalytic domain, exposing the active site for subsequent phosphorylation of other substrates (5).

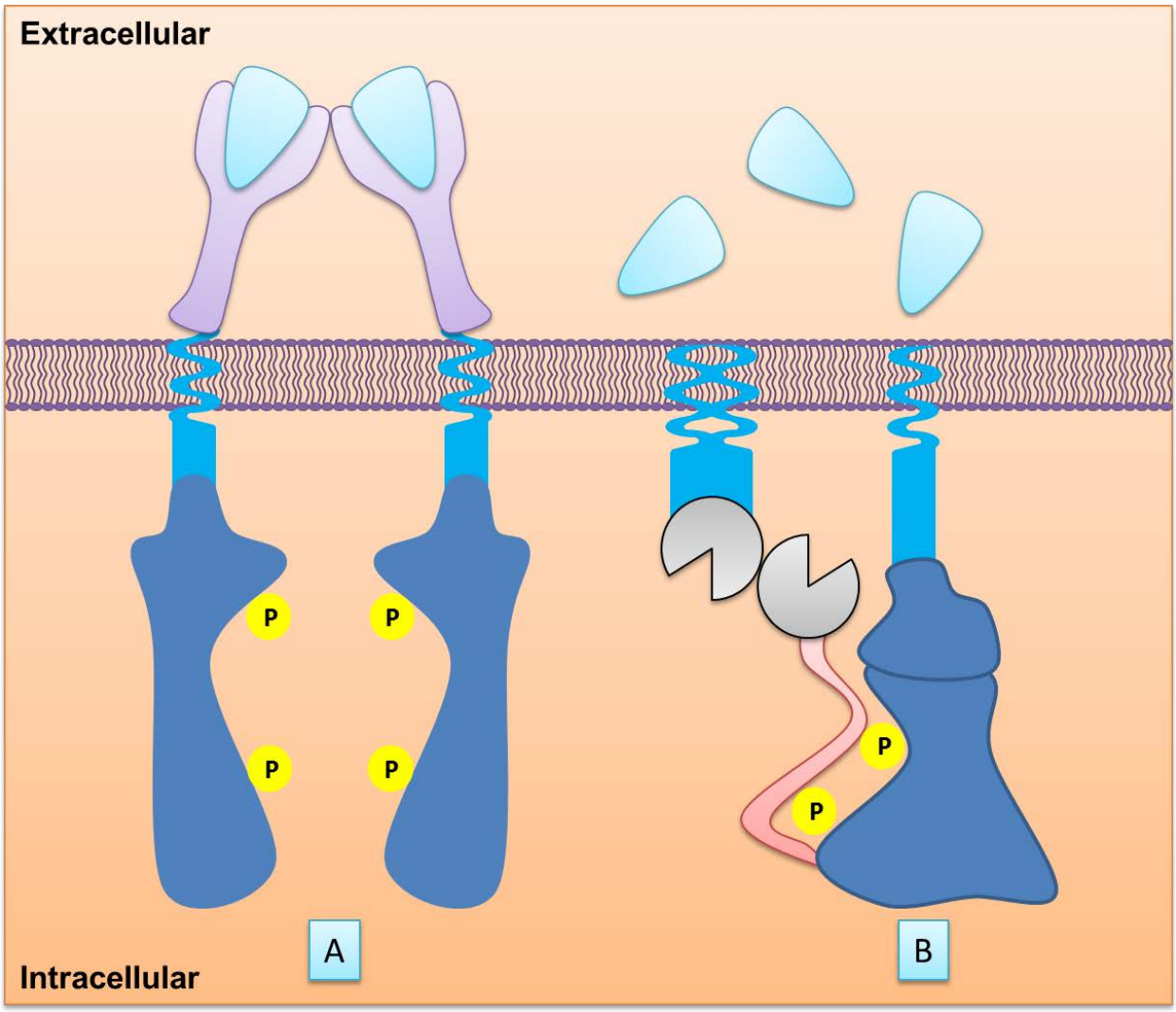

Figure 1.2 Cartoon depicting receptor and non-receptor tyrosine kinases. (A) Receptor tyrosine kinases (RTKs) are transmembrane proteins that require ligand binding and dimerization for activation. However, non-receptor tyrosine kinases (B) are cytosolic proteins that may or may not have membrane-associated components and rely on other kinases or phosphatases for activation.

Unlike RTKs, nonreceptor tyrosine kinases (nRTKs) do not contain extracellular ligand-binding domains and are mainly localized to the cytoplasm of cells (6). Nonreceptor tyrosine kinases are regulated by multiple intramolecular interactions that require a combination of phosphorylation and dephosphorylation events in order to assume the active conformation. In the Src-kinases for example, intramolecular interactions with the regulatory SH2 and SH3 domains force the kinase into a "compact," inactive form governed by the phosphorylation of a tyrosine residue at the 527 position (Tyr527). Upon dephosphorylation of Tyr527, the kinase unfolds and exposes yet another tyrosine residue at the 416 position, whose phosphorylation is necessary to stabilize the kinase in its active conformation (7, 8).

Many of the tyrosine kinases mediate signal transduction pathways that regulate a variety of different cellular processes including cell cycle progression, differentiation, and motility (9). Receptor tyrosine kinases of the EGFR family for example, have been found to regulate the transformation of cells from quiescence into the S-phase of the cell cycle, resulting in cell growth and differentiation (10, 11). Likewise the ABL1 kinase, an nRTK, was also shown to be involved in cell cycle regulation in response to DNA-damaging agents, through which it regulates DNA damage-repair events (12). Contrary to ABL1 however, the ABL2 kinase was shown to bind to actin and microtubules to aid in cytoskeletal functions, despite being in the same family as ABL1 (13). Although these kinases are subject to strict regulatory interactions, mutations in these regulatory elements can cause aberrant cell signaling and lead to uncontrolled cell growth and differentiation, which is a hallmark of many cancers.

Deregulation of Tyrosine Kinases in Cancer

In 2000, Hanahan and Weinberg noted that despite the complexity of cancer as a disease, many of the physiologic changes that occur during the transformation of normal cells to malignant cells aim to prolong survival and favor growth. They surmised that most, if not all cancers, displayed six general characteristics denoted as the "hallmarks of cancer." These hallmarks were defined as: evasion of apoptosis, self-sufficiency in growth signals, insensitivity to anti-growth signals, sustained angiogenesis, tissue invasion and metastasis, and limitless replicative potential (14). Hanahan and Weinberg then revisited these hallmarks in 2011 and proposed that in addition to these characteristics, a "tumor microenvironment" was also required for cancer progression. As such, they included the following as "emerging hallmarks and characteristics" that underlay the original six hallmarks and aid in tumoriogenesis: deregulation of cellular energetics, avoidance of immune destruction, genome instability and mutation, and tumor-promoting inflammation (15).

Although each of these processes are regulated by various kinases in a number of different pathways, the activation of these pathways is highly regulated by intramolecular interactions. Thus mutations in these regulatory elements would result in a constitutively active kinase such that proliferation and growth signals are propagated (16). One important structural regulatory element of tyrosine kinases is the juxtamembrane domain. In most tyrosine kinases, the juxtamembrane domain has been characterized as an auto-inhibitory regulatory domain whose phosphorylation is required to stabilize the kinase in an active state (17). Mutations that occur in the juxtamembrane domain can result in an activated kinase, without need for prior phosphorylation or ligand binding. In gastrointestinal stromal tumors for example, deletions and

substitutions in the juxtamembrane domain of KIT (a RTK) abolish its intramolecular auto-inhibitory mechanisms, allowing KIT to activate independent of ligand binding (18, 19).

The activation loop in tyrosine kinases also serves as an auto-regulatory mechanism by stabilizing the kinase in an inactive, "closed" form until key tyrosine residues within the loop are phosphorylated. Upon activation one or more tyrosine residues within the activation loop are trans-phosphorylated, which causes the loop to reposition and switch to an "open" conformation that increases access to ATP and substrate (20, 21). Mutations in the activation loop of the Fms-like tyrosine kinase 3 (FLT3), for example, have been shown *in vitro* to allow FLT3 to activate without ligand binding as measured by auto-phosphorylated FLT3 and activated downstream effectors (22). Interestingly, although most tyrosine kinases require phosphorylation of activation loop tyrosine residues for catalytic activity, mutations affecting conserved tyrosine residues in the activation loop of EGFR do not impact its activation and signaling, suggesting that the loop does not play a critical role in EGFR autoinhibition (23).

Although not considered to be an auto-inhibitory mechanism, the transmembrane domain of RTKs has been shown to impact catalytic activity due to their ability to stabilize the kinase upon ligand-dependent dimerization. In one proposed mechanism, the transmembrane domains of monomeric RTKs rotate their respective catalytic domains to an "open" form, which promotes phosphorylation between the two monomers upon dimerization (24). Pathogenic mutations in the transmembrane domains of RTKs can lead to aberrant signaling by overstabilizing the dimer, changing the membrane-embedded segment, or altering contact between extra- or intracellular domains of the dimers (4). However unlike the mutations in the extra- or intracellular domains, oncogenic mutations in transmembrane domains are relatively rare. The fibroblast growth factor receptor 3 (FGFR3) is known for having the highest number of pathogenic mutations in the

transmembrane domain (25) and it, along with other FGFRs (FGFR-1, -2, -4), are primarily important for skeletal system development (4). Although transmembrane domain mutations in FGFRs result in skeletal and cranial deformities, transmembrane and activating mutations specific to FGFR3 have been associated with bladder cancers (26) and multiple myeloma (27).

In addition to gain-of-function mutations in tyrosine kinases that can transform normal cells to malignant cells, chromosomal translocation events can result in the expression of a fusion protein that is constitutively active. Chromosomal translocations occur when a segment of one chromosome is transferred to either another chromosome or a different site on the same chromosome. Translocations do not often result in beneficial outcomes, have been shown to be associated with the disruption and misregulation of normal gene function, and have been linked to various cancers (28). The most notable example is the expression of the BCR-ABL fusion protein, which is the result of a reciprocal translocation between the breakpoint cluster region (BCR) gene on chromosome 22 and the ABL tyrosine kinase gene on chromosome 9 (29). This produces a truncated chromosome called the Philadelphia chromosome (Ph), named for its discovery by Nowell and Hungerford in the city of Philadelphia in 1960 (30). The BCR-ABL fusion protein is a deregulated nRTK whose activity promotes rapid proliferation, and is detected in patients with chronic myeloid leukemia (30) and some cases of acute lymphoblastic leukemia (31). In addition to BCR-ABL, fusion genes with other tyrosine kinases have been identified in other cancers including chronic myelomonocytic leukemia (Platelet Derived Growth Factor Receptor (PDGFR)-β, (32)) and more recently, non-small cell lung cancer (RET receptor, (33)).

Our increasing understanding of the underlying molecular mechanisms of cancer and the roles of tyrosine kinases further our ability to identify potential targets of therapy. The role of tyrosine kinases in cancer revolves around the propagation of intracellular signals to promote cell

growth and proliferation. Thus, uncovering kinases necessary for cancer initiation or progression, in addition to the mechanisms responsible for their deregulation, provides crucial data for the development of novel and selective inhibitors with which we can hope to better treat oncology patients.

ADVENT OF TARGETED THERAPIES

Prior to the implementation of targeted anticancer agents, cancers were often treated using cytotoxic chemotherapeutic drugs that aimed to kill rapidly dividing cells through a variety of mechanisms, depending on the class of drug used. Alkylating agents such as cyclophosphamide and chlorambucil, and platinum analogs including cisplatin and carboplatin, form adducts with DNA to prevent DNA synthesis and induce apoptosis. Antimetabolites (e.g. methotrexate, 5-fluorouracil, 6-mercaptopurine) were designed to mimic key endogenous molecules, such as folic acid, purines, and pyrimidines, which are necessary for nucleic acid and protein synthesis. Traditional chemotherapies also include hormonal analogs, such as anti-estrogens or anti-androgens, which block the activation of estrogen or androgen receptors in breast and prostate cancers, respectively (34).

Despite the efficaciousness of traditional chemotherapies, their use in clinical settings is often accompanied by a number of shortcomings. The most noticeable of these is the mechanism of action of these drugs, which does not distinguish normal from malignant cells. Consequentially, this results in the destruction of normal, rapidly dividing cells such as those found in bone marrow, hair, and the gastrointestinal lining, resulting in the most common adverse effects of traditional chemotherapy: immunosuppression, alopecia, and gastrointestinal distress (34). Additionally, traditional chemotherapies are often narrow therapeutic index drugs,

requiring careful monitoring of systemic concentrations and considerable dose adjustments to prevent added hepatic and renal toxicities.

Unlike traditional chemotherapies, the goal of targeted therapies is to selectively treat malignant cells apart from normal cells, giving them an added benefit in the treatment of various cancers. While traditional chemotherapies treat cancer by attacking rapidly dividing cells through the inhibition of cell division, targeted therapies block cell proliferation by interfering with specific cellular molecules required for growth that are often mutated or overexpressed in malignant cells (35). However, this can only be accomplished with sufficient knowledge about the molecular mechanisms behind cancer initiation and progression.

The identification of the Philadelphia chromosome and its role in chronic myeloid leukemia (CML) is a prime example of how targeting a molecular driver of a cancer can be an effective therapy. BCR-ABL, the gene product of the Philadelphia chromosome, is found in about 95% percent of patients diagnosed with CML, and numerous preclinical studies have shown that BCR-ABL inhibition via small molecule ATP-competitive inhibitors can induce apoptosis in leukemic cells expressing the protein (36-38). STI571, a 2-phenylaminopyrimidine derivative, was the product of rational drug design to develop selective inhibitors against BCR-ABL. In a phase I study conducted in Ph+ CML patients who have failed prior treatment with interferon-α (standard therapy), 98% of patients achieved a complete cytogenic response after four weeks of 300 mg or more STI571 given orally, once daily (39). Furthermore, another pilot study showed that STI571 can also induce cytogenic responses in patients with Ph+ CML in blast crisis (advanced form) or Ph+ acute lymphoblasic leukemia (40), providing further evidence for the potential usefulness of molecularly targeted therapies. Following these successes, STI571 was approved by the US Food and Drug Administration (FDA) in 2001 under

the name Gleevec (imatinib mesylate), for the treatment of Ph+ CML in blast crisis, accelerated phase, or chronic phase after interferon-α failure (41, 42).

Since the approval of imatinib in 2001, an increasing number of targeted therapies, both large and small molecules, have been approved by the FDA for a vast number of cancers. A list of approved and currently available targeted therapies for neoplastic diseases can be found in **Tables 1.1 and 1.2**.

Large molecule targeted therapies (**Table 1.1**) employ the use of monoclonal antibodies to selectively target cancer cells. These antibodies exert their pharmacologic action in various mechanisms, depending on the drug's target and must be given intravenously due to instability in the gastrointestinal tract. A major mechanism by which antibodies exert their pharmacologic effect is via antibody-dependent cell-mediated cytotoxicity (ADCC). In ADCC, antibodies first bind to extracellular molecules on the surface of cancer cells, effectively marking them for destruction. "Marked" cells are then attacked by various effector cells of the host immune system, including natural killer (NK) cells, macrophages, and eosinophils, leading to tumor cell apoptosis (43). Early examples of antibody therapy in cancer (e.g. rituximab, alemtuzumab) targeted various cell surface markers of differentiation, such as CD20 or CD52, to treat certain leukemias and lymphomas (44, 45). In addition to cell surface markers, RTKs can also be targeted in this fashion, as is the case for the anti-HER2 antibody, trastuzumab, which binds to overexpressed HER2 receptors in HER2+ breast cancers (46).

Table 1.1 Currently available monoclonal antibodies approved by the US Food & Drug Administrations for the treatment of neoplastic diseases

Drug	Trade Name	Company	Indication(s)	Target(s)	Year Approved
Rituximab	Rituxan	Genentech	Non-hodgkin's lymphoma, Chronic lymphocytic leukemia	CD20	1997
Trastuzumab	Herceptin	Genentech	Adjuvant breast cancer, Metastatic breast cancer, Metastatic gastric cancer	HER2	1998
Alemtuzumab	Campath	Genzyme	B-cell chronic lymphocytic leukemia	CD52	2001
Bevacizumab	Avastin	Genentech	Metastatic colorectal cancer, Non-squamous non-small cell lung cancer, Glioblastoma	VEGF	2004
Cetuximab	Erbitux	ImClone	Squamous cell carcinoma of the head and neck, K-RAS-/EGFR+ colorectal cancer	EGFR	2004
Panitumumab	Vectibix	Amgen	Metastatic colorectal cancer	EGFR	2006
Ofatumumab	Arzerra	GlaxoSmithKline	Untreated or refractory chronic lymphocytic leukemia	CD20	2009
Denosumab	Xgeva	Amgen	Bone metastasis from solid tumors, Giant cell tumor of bone	RANKL	2010
Brentuximab vedotin	Adcetris	Seattle Genetics	Hodgkin lymphoma, Systemic anaplastic large cell lymphoma	CD30	2011

Table 1.1 (continued)

Drug	Trade Name	Company	Indication(s)	Target(s)	Year Approved
Ipilimumab	Yervoy	Bristol Myers Squibb	Unresectable or metastatic melanoma	CTLA-4	2011
Pertuzumab	Perjeta	Genentech	Metastatic breast cancer, Neoadjuvant treatment of breast cancer	HER2	2012
Obinutuzumab	Gazyva	Genentech	Chronic lymphocytic leukemia	CD20	2013
Trastuzumab emtansine	Kadcyla	Genentech	HER2+ metastatic breast cancer	HER2	2013
Blinatumomab	Blincyto	Amgen	Ph- relapsed or refractory acute lymphoblastic leukemia	CD19	2014
Ramucirumab	Cyramza	Eli Lilly and Co.	Gastric cancer, Non-small cell lung cancer	VEGFR-2, VEGF-A/-C/-D	2014
Pembrolizumab	Keytruda	Merck Sharp & Dohme	Unresectable or metastatic melanoma	PD-1	2014
Nivolumab	Opdivo	Bristol Myers Squibb	Unresectable or metastatic melanoma	PD-1	2014

As an extension of this mechanism, antibody-drug conjugates (ADCs) are another form of targeted therapy that utilizes the preferential binding of an antibody to directly deliver cytotoxic agents (or payloads) to tumor cells. Cytotoxic agents are conjugated to antibodies with a linker that dissociates once the conjugate is internalized into tumor cells, thereby reducing the exposure of cytotoxic drugs to normal cells. However the development of ADCs still possesses a unique challenge as the correct antibody, linker, and cytotoxic agent must be selected to provide both selectivity and stability when given *in vivo* to avoid dissociation of payloads prior to reaching tumor cells (47, 48).

Monoclonal antibodies can also act as tyrosine kinase inhibitors (TKIs) either by binding to extracellular domains of RTKs or antagonizing their ligands. In doing so, these antibodies inhibit the ability of RTKs to dimerize, preventing the auto- or trans-phosphorylation events necessary for activation, thus inhibiting signals of proliferation (43). Pertuzumab for example, approved for the treatment of HER2+ metastatic breast cancer, binds to the extracellular domain of HER2 receptors expressed on tumor cells and prevents ligand-dependent dimerization of HER2 with other HER-type receptors necessary for catalytic activity (49).

Contrary to large molecule targeted therapies, small molecule TKIs target the intracellular catalytic domains of tyrosine kinases and compete with ATP to inhibit phosphorylation upon kinase activation (50). By targeting intracellular domains of mutated or overexpressed tyrosine kinases in malignant cells, small molecule TKIs have the capability to target both RTKs and nRTKs, although in each case the drug must first diffuse across the plasma membrane to do so. This nuance of small molecule TKIs is evident by the sheer number of drugs in this class that have been approved since imatinib's approval in 2001 (**Table 1.2**), as drug targets are not restricted to extracellular domains.

Table 1.2 Small molecule tyrosine kinase inhibitors approved by the US Food & Drug Administrations for the treatment of neoplastic diseases

Drug	Trade Name	Company	Indication	Targets	Year Approved
Imatinib	Gleevec	Novartis	Ph+ chronic myelogenous leukemia, Ph+ acute lymphoblastic leukemia	BCR-ABL, PDGFR, c-KIT	2003
Gefitinib	Iressa	AstraZeneca	Advanced or metastatic non-small cell lung cancer	EGFR	2003
Pegaptanib	Macugen	Valeant Pharmaceuticals	Neovascular age-related macular degeneration	VEGF antagonist	2004
Erlotinib	Tarceva	OSI Pharmaceuticals	Non-small cell lung cancer, Pancreatic cancer	EGFR	2004
Sorafenib	Nexavar	Bayer Healthcare	Hepatocellular/Renal cell/Differentiated thyroid carcinoma	BRAF, KIT, VEGFR-1/-2/-3	2005
Dasatinib	Sprycel	Bristol Myers Squibb	Ph+ chronic myelogenous leukemia, Ph+ acute lymphoblastic leukemia	BCR-ABL, Src-family kinases, PDGFR-β	2006
Sunitinib	Sutent	CPPI	Gastrointestinal stromal/Advanced pancreatic neuroendocrine tumors, Advanced renal cell carcinoma	PDGFR-α/-β, VEGFR-1/-2/-3, KIT	2006
Nilotinib	Tasigna	Novartis	Ph+ chronic myelogenous leukemia	BCR-ABL, PDGFR, c-KIT	2007
Lapatinib	Tykerb	SmithKline Beecham	HER2+ advanced or metastatic breast cancer	EGFR, HER2	2007

Table 1.2 (continued)

Drug	Trade Name	Company	Indication	Targets	Year Approved
Pazopanib	Votrient	GlaxoSmithKline	Advanced renal cell carcinoma, Advanced soft tissue sarcoma	VEGFR-1/-2/-3, PDGFR-α/-β, FGFR-1/-3	2009
Vandetanib	Caprelsa	IPR Pharmaceuticals	Medullary thyroid cancer	EGFR, VEGFR, Src-family kinases	2011
Ruxolitinib	Jakafi	Incyte	Myelofibrosis, Polycythemia vera	JAK1, JAK2	2011
Crizotinib	Xalkori	PF Prism CV	ALK+ metastatic non-small cell lung cancer	ALK, HGFR, ROS1	2011
Vemurafenib	Zelboraf	Hoffmann La Roche	Unresectable or metastatic melanoma with BRAF V600E mutation	BRAF V600E	2011
Bosutinib	Bosulif	Wyeth Pharmaceuticals	Ph+ chronic myelogenous leukemia	BCR-ABL, Src-family kinases (Src, Lyn, Hck)	2012
Vismodegib	Erivedge	Genentech	Metastatic basal cell carcinoma	Smoothened (Smo)	2012
Cabozantinib	Cometriq	Exelixis	Medullary thyroid cancer	RET, MET, VEGFR-1/-2/-3	2012
Ponatinib	Iclusig	Ariad	T315I+ chronic myelogenous leukemia, T315I-Ph+ acute lymphoblastic leukemia	ABL, T315I-mutated ABL, VEGFR, PDGFR, Src-family kinases	2012

Table 1.2 (continued)

Drug	Trade Name	Company	Indication	Targets	Year Approved
Axitinib	Inlyta	Pfizer	Advanced renal cell carcinoma	VEGFR-1/-2/-3	2012
Regorafenib	Stivarga	Bayer Healthcare	Colorectal cancer, Gastrointestinal stromal tumors	RET, KIT, VEGFR-1/-2/-3	2012
Tofacitinib	Xeljanz	PF Prism CV	Rheumatoid arthritis	JAK-family kinases	2012
Afatinib	Gilotrif	Boehringer Ingelheim	Metastatic non-small cell lung cancer	EGFR, HER2, HER4	2013
Trametinib	Mekinist	GlaxoSmithKline	Unresectable or metastatic melanoma with BRAF V600E or V600K mutations	MEK-1/-2	2013
Dabrafenib	Tafinlar	GlaxoSmithKline	Unresectable or metastatic melanoma with BRAF V600E or V600K mutations	BRAF V600E/V600K/V600D	2013
Ibrutinib	Imbruvica	Pharmacyclics	Mantle cell lymphoma, Chronic lymphocytic leukemia	BTK	2014
Nintendanib	Ofev	Boehringer Ingelheim	Idiopathic pulmonary fibrosis	PDGFR-α/-β, VEGFR-1/-2/-3, FGFR-1/-2/-3	2014
Certinib	Zykadia	Novartis	ALK+ metastatic non-small cell lung cancer	ALK, IGF-1R, ROS1	2014
Lenvatinib	Lenvima	Eisai	Refractory thyroid cancer	VEGFR-1/-2/-3	2015

Small molecule TKIs also have the capability to simultaneously target multiple tyrosine kinases expressed for a particular cancer. Although this may initially appear as a lack of sensitivity, many have argued that this approach favors targeted therapies due the heterogeneity of cancer (51-53). The aim of TKI therapy is to inhibit the propagation of growth and proliferation signals in malignant cells and due to the complexity of these signaling pathways, attacking multiple targets may provide added coverage for potential compensatory or escape mechanisms by which a malignant cell can override the effects of inhibition (53). However, this strategy is not simply limited to TKIs, as it also applies to combinations of other targeted therapies with traditional chemotherapeutics. A number of targeted therapies have been approved by the FDA in recent years for use in combinations with traditional chemotherapeutics, including the ramicirumab/docetaxel combination for non-small cell lung cancer and the bevacizumab/paclitaxel combination for metastatic cervical cancer, both of which were approved in 2014 (54).

Our increasing understanding of the molecular mechanisms of cancer has led to the advent of targeted therapies and a shift in the paradigm of how oncology patients are treated. Despite the successes of these targeted therapies however, traditional chemotherapies are still valuable particularly for their use in combination with targeted agents or for those cancers that lack suitable or druggable targets.

Challenges in the Development of Targeted Therapies

The drug development process is by no means an easy one. According to a 2014 report from the Pharmaceutical Research and Manufacturers of America (PhRMA), the estimated time to develop a drug ranges between 10-15 years and costs an average of $1.2 billion, including the

cost of failures (55). Furthermore, attrition rates in oncology drug development are reportedly much higher than other therapeutic areas, with approximately only 5% of new molecular entities with anticancer activity receiving approval after phase III clinical trials (56). Among the multitude of factors that influence the development of targeted therapies, the most impactful are target identification and drug resistance (56-58).

The identification of appropriate targets during the development of targeted anticancer agents requires an advanced understanding of the molecular drivers of the cancer. In the case of the Philadelphia chromosome and its role in CML described above, much of the success of imatinib therapy comes from the discovery that almost all CML patients possess the Philadelphia chromosome and inhibition of its gene product, BCR-ABL, resulted in the induction of apoptosis in leukemic cells (36, 59). However, most other cancers often possess multiple factors that influence cancer progression and in these circumstances, what becomes equally as important as the identity of these factors is the significance of their activity to disease (52).

In conjunction with the characterization of potential targets, the validity of these targets and the ability to test them in the appropriate preclinical models was also common among reports of attrition rates in oncology drug development, due to the inability of preclinical models to accurately predict efficacy and toxicity in humans. Many of the arguments have ranged from the inherent limitations of preclinical (i.e. animal) models to accurately represent the tumor micro-environments and human disease progression, to the lack of reproducibility of reported data in the scientific literature, which serves as the basis for the design of many preclinical studies (58, 60, 61). The use of phase 0 studies in humans has also been proposed as a means to evaluate the ability of an anticancer agent to modulate the correct molecular target (i.e. mechanism of action) and accelerate oncology drug development (61). However, as these studies are done in a small

subset of patients and have no intent to provide any therapeutic benefit, caution must be taken to avoid potential exclusion of these patients from participating in other clinical studies where a therapeutic benefit may occur (62).

Next to target identification and validation however, the biggest adversary to the development of targeted therapies is drug resistance. Drug resistance is classified as either intrinsic, in which cancer cells inherently possess traits that would confer resistance without exposure to drug, or acquired, which is sometimes described as an adaptive ability by the cancer cell to develop resistance mechanisms post-exposure to drug (63). Drug resistance is conferred through a variety of different mechanisms and can develop when a subpopulation of resistant cells overpopulate nonresistant cells in the tumor by therapy-induced selection.

One particular mechanism of resistance impacts the pharmacokinetics and pharmacodynamics of anticancer agents at the site of action. The overexpression of efflux transporters, such as P-glycoprotein (P-gp) or Breast Cancer Resistant Protein (BCRP), limit the exposure of tumor cells to cytotoxic drugs by pumping them out of the cell upon entry, as is the case for many traditional chemotherapies including docetaxel, cisplatin, and irenotecan (64). Drug resistance can also develop through the reduction of cellular uptake mechanisms mediated by uptake transporters or via endocytosis (65). These mechanisms, especially common to traditional chemotherapies, reduce intracellular concentrations of drug in tumor cells and prevent cytotoxicity.

Drug resistance can also occur through compensatory mechanisms, such as the overexpression of targets (receptors or ligands) or the activation of downstream signaling pathways. The antimetabolite 5-fluorouracil (5-FU), which is used to treat various cancers including colorectal, head and neck cancers, is metabolized to several active metabolites that

inhibit thymidylate synthase. Thymidylate synthase is responsible for the production of thymidine, which is necessary for DNA synthesis and repair and was found to be overexpressed in resistant colorectal cancers (66). In another case, resistance to trastuzumab therapy can develop in HER2+ breast cancers via a number of proposed mechanisms, including the presence of activating mutations in the PI3K/mTOR signaling pathways, both of which are downstream of the HER2 receptor and are implicated in the pathogenesis of a number of other cancers as well (67).

A major mechanism of drug resistance, particularly for small molecule TKIs, is the development of gatekeeper residue mutations in tyrosine kinases. Gatekeeper residues are single residues that regulate the interactions of inhibitors with a hydrophobic pocket located deep in the ATP-binding site, and mutations in these residues reduce the affinity of the TKI for the ATP-binding site and decrease efficacy. Gatekeeper mutations were first identified in patients with Ph+ CML, which conferred resistance to imatinib therapy. The T315I mutation occurs in the ABL sequence of the BCR-ABL gene and prevents imatinib binding via steric hindrance and the removal of a critical hydrogen binding interaction, while still maintaining the kinase's catalytic activity (68). However, this particular mutation also confers resistance against other BCR-ABL inhibitors, including dasatinib, nilotinib, bosutinib, all of which are more potent inhibitors of BCR-ABL relative to imatinib (69). In spite of these mutations, new BCR-ABL inhibitors have shown promise against Ph+ CML and Ph+ ALL with the T315I mutation, most notably ponatinib, which was approved by the FDA in 2012.

Gatekeeper mutations have also been identified in patients with non-small cell lung cancer. A previous study reported that 55% of patients with EGFR mutations responded to gefitinib therapy, with a median progression-free survival of 9.2 months (70). However,

resistance to EGFR inhibitors (e.g. gefitinib, erlotinib) often develops due to the T790M gatekeeper mutation, which is found in over 50% of EGFR mutants with acquired drug resistance (71). In this case, a beneficial strategy for treatment would be to either challenge the tumor with other TKIs or consider the use of monoclonal antibodies (72).

Other Considerations

Other points of consideration regarding the use and development of targeted therapies include personalized medicine, appropriate clinical trial design and endpoints, and the influence of variability on therapeutic efficacy.

The idea of personalized medicine in the oncology setting certainly seems achievable given our increasing understanding of cancer initiation and progression. Furthermore, with the ability to identify a specific subtype of cancer at a molecular level, this knowledge can provide crucial insights to selecting the appropriate drug or drug combination for a specific patient. This is particularly beneficial for breast cancers for example, which have a number of different subtypes (endocrine receptor positive, HER2 positive, triple positive, and triple negative) each requiring different anticancer agents and forms of treatment.

Proper clinical trial design and endpoint selection is also another point of consideration in the development of targeted therapies. In the 2007 guidance for industry on clinical trial endpoints, overall survival is defined as the time from randomization until death from any cause and is measured in the intent-to-treat population (73). Overall survival is viewed as the gold standard of oncology clinical trial endpoints as it is the least ambiguous to measure and least impacted by investigator bias. However, this may not necessarily be the ideal endpoint in all cases, as a complete assessment of overall survival would often require larger sample sizes and

longer periods of follow-up. The use of surrogate endpoints in early clinical trials may be beneficial in providing information regarding the pharmacologic activity of a drug, but the usage of surrogate endpoints for drug approval requires rigorous validation of the surrogate used (analogous to target identification).

Last, patient variability in both pharmacokinetics and pharmacodynamics can directly impact the use of targeted therapies in the clinical setting. Although the variability in response to targeted therapies may be attributed in part to the heterogeneity of cancer, variability in the pharmacokinetics of these drugs can be attributed to ADME (absorption, distribution, metabolism, excretion) processes that dictate systemic exposure of drugs. Concomitant medications in oncology can represent a large portion of pharmacokinetic variability for example, because of potential drug-drug interactions that may induce or inhibit drug metabolizing enzymes and/or transporters (74).

CONCLUSIONS

Our understanding of the molecular mechanisms of cancer and the roles that tyrosine kinases have in cancer initiation and progression have led to the emergence and success of targeted anticancer therapies, greatly improving the prognoses of numerous cancers. Although the development of future targeted therapies is challenged by identifying druggable targets and overcoming drug resistance, the combination of targeted therapies and traditional chemotherapeutics may provide potentially beneficial treatment strategies for patients whose cancers have already acquired drug resistance. Thus the continued evolution of cancer therapies and use in clinical settings will aid in shifting the view of cancer from a deadly, debilitating disease, to a chronic, more manageable health condition.

GOALS AND AIMS OF THESIS WORK

As the therapeutic efficacy of a drug is driven by its pharmacokinetics, the goal of this work was to evaluate potential mechanisms by which TKI drug exposure can be altered. Many TKIs are weakly basic drugs with pH-dependent solubility and exhibit a significantly reduced solubility at elevated pH. Furthermore, TKIs are extensively metabolized in the liver by phase I and phase II metabolic processes and are dependent on metabolism for elimination from the body. In addition, previous studies from our laboratory have shown that mechanisms of hepatic uptake (i.e. via uptake transporters) can greatly influence hepatic clearance mechanisms, which may have consequences on drug exposure. We hypothesize therefore, that the drug disposition of small molecule TKIs can be affected by gastric pH and hepatic uptake transporters, which are viable targets for potential drug-drug interactions that may result in significant changes in TKI drug exposure.

Because of their pH-dependent solubility, many acid-reducing agents (ARAs), such as proton pump inhibitors (PPIs) and H_2-receptor antagonists (H2RAs), are not recommended to be taken concomitantly with small molecule TKIs due to the elevation of fasting gastric pH upon chronic ARA administration (hypochlorhydria). Dasatinib (Sprycel) is an example of such a drug and has been previously shown to exhibit significantly reduced drug exposures when coadministered with the H2RA, famotidine. In a two-part clinical study, we first evaluate the ability of betaine hydrochloride, a nutraceutical used as a digestive aid, to artificially reacidify gastric pH in healthy volunteers with rabeprazole (a PPI)-induced hypochlorhydria. In a follow-up study, we then evaluate the effects of gastric pH on dasatinib pharmacokinetics, proposing the use of betaine hydrochloride as a potential mitigation strategy for small molecule anticancer agents hindered by pH-dependent solubility and frequently coadministered with ARAs.

We then evaluate the roles of hepatic uptake transporters on drug disposition of three selected TKIs due to their dependence on hepatic metabolism for drug elimination. We employ the use of the Biopharmaceutics Drug Disposition Classification System (BDDCS), which categorizes drugs into four classes based on their solubility, extent of metabolism, and intestinal permeability rate, and can be used to predict the effects of drug-drug interactions mediated by uptake or efflux transporters. *In vitro* permeability methods are used to experimentally define BDDCS class followed by the use of transfected cellular models and cryopreserved human hepatocytes to evaluate the effects of the inhibition of four human hepatic uptake transporters: Organic Cation Transporter 1 (OCT1), Organic Anion Transporting Polypeptide-1B1, -1B3, and -2B1 (OATP1B1, -1B3, -2B1).

Collectively, this work aims to highlight potentially significant areas of focus in the drug development of TKIs, focusing mainly on gastric pH and hepatic uptake transporters due to their importance in ADME processes. The results of the research presented herein hopes to aid in the production of more beneficial targeted therapies that may translate to more effective treatments for oncology patients.

REFERENCES

1. Manning G, Whyte DB, Martinez R, Hunter T, Sudarsanam S. The protein kinase complement of the human genome. Science. 2002;298:1912-34.
2. Kimura T, Sakamoto H, Appella E, Siraganian RP. Conformational changes induced in the protein tyrosine kinase p72syk by tyrosine phosphorylation or by binding of phosphorylated immunoreceptor tyrosine-based activation motif peptides. Mol Cell Biol. 1996;16:1471-8.
3. Hubbard SR, Miller WT. Receptor tyrosine kinases: mechanisms of activation and signaling. Curr Opin Cell Biol. 2007;19:117-23.
4. Li E, Hristova K. Receptor tyrosine kinase transmembrane domains: Function, dimer structure and dimerization energetics. Cell Adh Migr. 2010;4:249-54.
5. Linggi B, Carpenter G. ErbB receptors: new insights on mechanisms and biology. Trends Cell Biol. 2006;16:649-56.
6. Neet K, Hunter T. Vertebrate non-receptor protein-tyrosine kinase families. Genes Cells. 1996;1:147-69.
7. Roskoski R, Jr. Src protein-tyrosine kinase structure and regulation. Biochem Biophys Res Commun. 2004;324:1155-64.
8. Filippakopoulos P, Muller S, Knapp S. SH2 domains: modulators of nonreceptor tyrosine kinase activity. Curr Opin Struct Biol. 2009;19:643-9.
9. Bhise SB, Nalawade AD, Wadhawa H. Role of protein tyrosine kinase inhibitors in cancer therapeutics. Indian J Biochem Biophys. 2004;41:273-80.
10. Paul MK, Mukhopadhyay AK. Tyrosine kinase - Role and significance in Cancer. Int J Med Sci. 2004;1:101-15.

11. Arora A, Scholar EM. Role of tyrosine kinase inhibitors in cancer therapy. J Pharmacol Exp Ther. 2005;315:971-9.

12. Yuan ZM, Huang Y, Whang Y, Sawyers C, Weichselbaum R, Kharbanda S, et al. Role for c-Abl tyrosine kinase in growth arrest response to DNA damage. Nature. 1996;382:272-4.

13. Colicelli J. ABL tyrosine kinases: evolution of function, regulation, and specificity. Sci Signal. 2010;3:re6.

14. Hanahan D, Weinberg RA. The hallmarks of cancer. Cell. 2000;100:57-70.

15. Hanahan D, Weinberg RA. Hallmarks of cancer: the next generation. Cell. 2011;144:646-74.

16. Vlahovic G, Crawford J. Activation of tyrosine kinases in cancer. Oncologist. 2003;8:531-8.

17. Hubbard SR. Juxtamembrane autoinhibition in receptor tyrosine kinases. Nat Rev Mol Cell Biol. 2004;5:464-71.

18. Hirota S, Isozaki K, Moriyama Y, Hashimoto K, Nishida T, Ishiguro S, et al. Gain-of-function mutations of c-kit in human gastrointestinal stromal tumors. Science. 1998;279:577-80.

19. Chan PM, Ilangumaran S, La Rose J, Chakrabartty A, Rottapel R. Autoinhibition of the kit receptor tyrosine kinase by the cytosolic juxtamembrane region. Mol Cell Biol. 2003;23:3067-78.

20. Hubbard SR. Protein tyrosine kinases: autoregulation and small-molecule inhibition. Curr Opin Struct Biol. 2002;12:735-41.

21. Schlessinger J. Ligand-induced, receptor-mediated dimerization and activation of EGF receptor. Cell. 2002;110:669-72.

22. Clark JJ, Cools J, Curley DP, Yu JC, Lokker NA, Giese NA, et al. Variable sensitivity of FLT3 activation loop mutations to the small molecule tyrosine kinase inhibitor MLN518. Blood. 2004;104:2867-72.

23. Gotoh N, Tojo A, Hino M, Yazaki Y, Shibuya M. A highly conserved tyrosine residue at codon 845 within the kinase domain is not required for the transforming activity of human epidermal growth factor receptor. Biochem Biophys Res Commun. 1992;186:768-74.

24. Li E, Hristova K. Role of receptor tyrosine kinase transmembrane domains in cell signaling and human pathologies. Biochemistry. 2006;45:6241-51.

25. Sarabipour S, Hristova K. FGFR3 transmembrane domain interactions persist in the presence of its extracellular domain. Biophys J. 2013;105:165-71.

26. Otsuki T, Nakazawa N, Taniwaki M, Yamada O, Sakaguchi H, Wada H, et al. Establishment of a new human myeloma cell line, KMS-18, having t(4;14)(p16.3;q32.3) derived from a case phenotypically transformed from Ig A-lambda to BJP-lambda, and associated with hyperammonemia. Int J Oncol. 1998;12:545-52.

27. van Rhijn BW, van Tilborg AA, Lurkin I, Bonaventure J, de Vries A, Thiery JP, et al. Novel fibroblast growth factor receptor 3 (FGFR3) mutations in bladder cancer previously identified in non-lethal skeletal disorders. Eur J Hum Genet. 2002;10:819-24.

28. O'Connor C. Human chromosome translocations and cancer. Nature Education. 2008;1:56.

29. Rowley JD. Letter: A new consistent chromosomal abnormality in chronic myelogenous leukaemia identified by quinacrine fluorescence and Giemsa staining. Nature. 1973;243:290-3.

30. Nowell P, Hungerford D. A minute chromosome in human chronic granulocytic leukemia [abstract]. Science. 1960;132:1497.

31. Fielding AK. Current treatment of Philadelphia chromosome-positive acute lymphoblastic leukemia. Haematologica. 2010;95:8-12.

32. Golub TR, Barker GF, Lovett M, Gilliland DG. Fusion of PDGF receptor beta to a novel ets-like gene, tel, in chronic myelomonocytic leukemia with t(5;12) chromosomal translocation. Cell. 1994;77:307-16.

33. Qian Y, Chai S, Liang Z, Wang Y, Zhou Y, Xu X, et al. KIF5B-RET fusion kinase promotes cell growth by multilevel activation of STAT3 in lung cancer. Mol Cancer. 2014;13:176.

34. Chabner BA. General principles of cancer chemotherapy. In: Brunton LL, Chabner BA, Knollmann BC, editors. Goodman & Gilman's The Pharmacological Basis of Therapeutics. 12th ed [Internet]. New York: McGraw-Hill [cited February 20, 2015]. Available from: http://accessmedicine.mhmedical.com/content.aspx?bookid=374&Sectionid=41266272. Subcription required to view.

35. Gerber DE. Targeted therapies: a new generation of cancer treatments. Am Fam Physician. 2008;77:311-9.

36. Druker BJ, Tamura S, Buchdunger E, Ohno S, Segal GM, Fanning S, et al. Effects of a selective inhibitor of the Abl tyrosine kinase on the growth of Bcr-Abl positive cells. Nat Med. 1996;2:561-6.

37. Gambacorti-Passerini C, le Coutre P, Mologni L, Fanelli M, Bertazzoli C, Marchesi E, et al. Inhibition of the ABL kinase activity blocks the proliferation of BCR/ABL+ leukemic cells and induces apoptosis. Blood Cells Mol Dis. 1997;23:380-94.

38. le Coutre P, Mologni L, Cleris L, Marchesi E, Buchdunger E, Giardini R, et al. In vivo eradication of human BCR/ABL-positive leukemia cells with an ABL kinase inhibitor. J Natl Cancer Inst. 1999;91:163-8.

39. Druker BJ, Talpaz M, Resta DJ, Peng B, Buchdunger E, Ford JM, et al. Efficacy and safety of a specific inhibitor of the BCR-ABL tyrosine kinase in chronic myeloid leukemia. N Engl J Med. 2001;344:1031-7.

40. Druker BJ, Sawyers CL, Kantarjian H, Resta DJ, Reese SF, Ford JM, et al. Activity of a specific inhibitor of the BCR-ABL tyrosine kinase in the blast crisis of chronic myeloid leukemia and acute lymphoblastic leukemia with the Philadelphia chromosome. N Engl J Med. 2001;344:1038-42.

41. Charatan F. US approves new anti-leukaemia drug. BMJ. 2001;322:1201.

42. US Food and Drug Administration. Imatinib (Gleevec) Prescribing Information. 2001.

43. Adams GP, Weiner LM. Monoclonal antibody therapy of cancer. Nat Biotechnol. 2005;23:1147-57.

44. Fang D, Nguyen TK, Leishear K, Finko R, Kulp AN, Hotz S, et al. A tumorigenic subpopulation with stem cell properties in melanomas. Cancer Res. 2005;65:9328-37.

45. Enblad G, Hagberg H, Erlanson M, Lundin J, MacDonald AP, Repp R, et al. A pilot study of alemtuzumab (anti-CD52 monoclonal antibody) therapy for patients with relapsed or chemotherapy-refractory peripheral T-cell lymphomas. Blood. 2004;103:2920-4.

46. Vu T, Claret FX. Trastuzumab: updated mechanisms of action and resistance in breast cancer. Front Oncol. 2012;2:62.

47. Feld J, Barta SK, Schinke C, Braunschweig I, Zhou Y, Verma AK. Linked-in: design and efficacy of antibody drug conjugates in oncology. Oncotarget. 2013;4:397-412.

48. Bouchard H, Viskov C, Garcia-Echeverria C. Antibody-drug conjugates-A new wave of cancer drugs. Bioorg Med Chem Lett. 2014;24:5357-63.

49. Phillips GD, Fields CT, Li G, Dowbenko D, Schaefer G, Miller K, et al. Dual targeting of HER2-positive cancer with trastuzumab emtansine and pertuzumab: critical role for neuregulin blockade in antitumor response to combination therapy. Clin Cancer Res. 2014;20:456-68.

50. Krause DS, Van Etten RA. Tyrosine kinases as targets for cancer therapy. N Engl J Med. 2005;353:172-87.

51. Faivre S, Djelloul S, Raymond E. New paradigms in anticancer therapy: targeting multiple signaling pathways with kinase inhibitors. Semin Oncol. 2006;33:407-20.

52. Broekman F, Giovannetti E, Peters GJ. Tyrosine kinase inhibitors: Multi-targeted or single-targeted? World J Clin Oncol. 2011;2:80-93.

53. Zhou C. Multi-targeted tyrosine kinase inhibitors for the treatment of non-small cell lung cancer: an era of individualized therapy. Transl Lung Cancer Res. 2012;1:72-7.

54. US Food and Drug Administration. Hematology/Oncology (Cancer) Approvals & Safety Notifications [cited 2015 02/27]. Available from: http://www.fda.gov/Drugs/InformationOnDrugs/ApprovedDrugs/ucm279174.htm.

55. Pharmaceutical Research and Manufactureres of America. 2014 biopharmaceutical research industry profile. 2014.

56. Hutchinson L, Kirk R. High drug attrition rates--where are we going wrong? Nat Rev Clin Oncol. 2011;8:189-90.

57. Kola I, Landis J. Can the pharmaceutical industry reduce attrition rates? Nat Rev Drug Discov. 2004;3:711-5.

58. Stock JK, Jones NP, Hammonds T, Roffey J, Dillon C. Addressing the right targets in oncology: challenges and alternative approaches. J Biomol Screen. 2015;20:305-17.

59. Shah NP, Kasap C, Weier C, Balbas M, Nicoll JM, Bleickardt E, et al. Transient potent BCR-ABL inhibition is sufficient to commit chronic myeloid leukemia cells irreversibly to apoptosis. Cancer Cell. 2008;14:485-93.

60. Begley CG, Ellis LM. Drug development: Raise standards for preclinical cancer research. Nature. 2012;483:531-3.

61. Mak IW, Evaniew N, Ghert M. Lost in translation: animal models and clinical trials in cancer treatment. Am J Transl Res. 2014;6:114-8.

62. Marchetti S, Schellens JH. The impact of FDA and EMEA guidelines on drug development in relation to Phase 0 trials. Br J Cancer. 2007;97:577-81.

63. Holohan C, Van Schaeybroeck S, Longley DB, Johnston PG. Cancer drug resistance: an evolving paradigm. Nat Rev Cancer. 2013;13:714-26.

64. Thomas H, Coley HM. Overcoming multidrug resistance in cancer: an update on the clinical strategy of inhibiting p-glycoprotein. Cancer Control. 2003;10:159-65.

65. Shen DW, Pouliot LM, Hall MD, Gottesman MM. Cisplatin resistance: a cellular self-defense mechanism resulting from multiple epigenetic and genetic changes. Pharmacol Rev. 2012;64:706-21.

66. Peters GJ, Backus HH, Freemantle S, van Triest B, Codacci-Pisanelli G, van der Wilt CL, et al. Induction of thymidylate synthase as a 5-fluorouracil resistance mechanism. Biochim Biophys Acta. 2002;1587:194-205.

67. O'Brien NA, McDonald K, Tong L, von Euw E, Kalous O, Conklin D, et al. Targeting PI3K/mTOR overcomes resistance to HER2-targeted therapy independent of feedback activation of AKT. Clin Cancer Res. 2014;20:3507-20.

68. Bixby D, Talpaz M. Mechanisms of resistance to tyrosine kinase inhibitors in chronic myeloid leukemia and recent therapeutic strategies to overcome resistance. Hematology Am Soc Hematol Educ Program. 2009:461-76.

69. Modugno M. New resistance mechanisms for small molecule kinase inhibitors of Abl kinase. Drug Discov Today Technol. 2014;11:5-10.

70. Sequist LV, Martins RG, Spigel D, Grunberg SM, Spira A, Janne PA, et al. First-line gefitinib in patients with advanced non-small-cell lung cancer harboring somatic EGFR mutations. J Clin Oncol. 2008;26:2442-9.

71. Denis MG, Vallee A, Theoleyre S. EGFR T790M resistance mutation in non small-cell lung carcinoma. Clin Chim Acta. 2015;444C:81-5.

72. Matikas A, Mistriotis D, Georgoulias V, Kotsakis A. Current and future approaches in the management of non-small-cell lung cancer patients with resistance to EGFR TKIs. Clin Lung Cancer. Epub ahead of print. January 8, 2015.

73. US Food and Drug Administration, Center for Drug Evaluation and Research and Center for Biologics Evaluation and Research. Guidance for industry - Clinial trial endpoints for the approval of cancer drugs and biologics. 2007.

74. Di Gion P, Kanefendt F, Lindauer A, Scheffler M, Doroshyenko O, Fuhr U, et al. Clinical pharmacokinetics of tyrosine kinase inhibitors: focus on pyrimidines, pyridines and pyrroles. Clin Pharmacokinet. 2011;50:551-603.

CHAPTER 2. GASTRIC RE-ACIDIFICATION WITH BETAINE HCL IN HEALTHY VOLUNTEERS WITH RABPERAZOLE-INDUCED HYPOCHLORHYDRIA*

ABSTRACT

Previous studies have demonstrated that increased gastric pH from the use of acid-reducing agents, such as proton-pump inhibitors or H_2-receptor antagonists, can significantly impact the absorption of weakly basic drugs that exhibit pH-dependent solubility. Clinically practical strategies to mitigate this interaction have not been developed. This pilot study evaluated the extent and time course of gastric re-acidification after a solid oral dosage form of anhydrous betaine HCl in healthy volunteers with pharmacologically-induced hypochlorhydria. Six healthy volunteers with baseline normochlorhydria (fasting gastric pH < 4) were enrolled in this single period study. Hypochlorhydria was induced via 20 mg oral rabeprazole twice daily for four days. On the fifth day, an additional 20 mg dose of oral rabeprazole was given and gastric pH was monitored continuously using the Heidelberg pH capsule. After gastric pH > 4 was confirmed for 15 minutes, 1500 mg of betaine HCl was given orally with 90 mL of water and gastric pH was continuously monitored for 2 hours. Betaine HCl significantly lowered gastric pH by 4.5 (±0.5) units from 5.2 (±0.5) to 0.6 (±0.2) (P <0.001) during the 30 minute interval after administration. The onset of effect of betaine HCl was rapid, with a mean time to pH < 3 of 6.3 (±4.3) minutes. The re-acidification period was temporary with a gastric pH < 3 and < 4 lasting 73 (±33) and 77 (±30) minutes, respectively. Betaine HCl was well tolerated by all subjects. In healthy volunteers with pharmacologically-induced hypochlorhydria, betaine HCl

*Modified from publication: Yago MR, Frymoyer AR, Smelick GS, Frassetto LA, Budha NR, Dresser MJ, et al. Gastric reacidification with betaine HCl in healthy volunteers with rabeprazole-induced hypochlorhydria. Mol Pharm. 2013; 10:4032-7.

was effective at temporarily lowering gastric pH. The rapid onset and relatively short duration of gastric pH reduction gives betaine HCl the potential to aid the absorption of orally administered weakly basic drugs that exhibit pH-dependent solubility when administered under hypochlorhydric conditions.

INTRODUCTION

Previous studies have investigated the effects of gastric pH on the absorption of orally administered drugs (1-3), emphasizing the importance of gastric acid to the dissolution and solubilization processes. These pH effects on absorption are also dependent on the physicochemical properties of each individual compound, such as native ionic state, acid dissociation constants (pK_a), and partition coefficient (logP). Moreover, the magnitude of these effects can be amplified for compounds that exhibit pH-dependent solubility, where exponential changes in solubility are observed as the pH rises or falls.

This gastric pH interaction is highlighted for weakly-basic drugs that exhibit decreasing solubility over the pH range 1 to 4, as elevations in gastric pH reduce the solubility of these drugs and can lead to reduced drug absorption and systemic exposure. An example of such a compound is atazanavir, which is a protease inhibitor that is weakly basic with a pK_a of 4.25 (4). When administered in the presence of a low dose of omeprazole (20 mg orally), atazanavir area under the plasma concentration-time curve (AUC_{0-24}) and trough levels (C_{min}) were reduced by 42% (90% CI of geometric mean ratio: 0.44-0.75) and 46% (90% CI of geometric mean ratio: 0.41-0.71), respectively (5). Many synthetic triazole antifungal agents are also weak bases with pH-dependent solubility and are affected by elevations in gastric pH. Itraconazole for example, which has a pK_a of 3.7 (6), showed significant reductions in plasma AUC_{0-24} and maximum plasma concentration (C_{max}) of 64% and 66% ($P < 0.05$), respectively, when administered to healthy volunteers pre-treated with oral omeprazole (40 mg daily) for 14 days (7). In a similar fashion, ketoconazole, when co-administered with cimetidine, suffered reductions in AUC and C_{max} of greater than 90% in healthy volunteers (8).

In an attempt to mitigate the impact of acid-reducing agents on drug absorption for weakly-basic drugs with pH-dependent solubility, Chin *et al.* (1) conducted a prospective clinical study investigating the effects of an acidic beverage (Coca-Cola®) on the pharmacokinetics of ketoconazole. When ketoconazole was dosed with Coca-Cola® (pH = 2.5) under the effects of omeprazole, ketoconazole $AUC_{0-\infty}$ and C_{max} were both increased by greater than 10-fold when compared to the omeprazole treatment without Coca-Cola® (1), though Coca-Cola® did not completely restore the omeprazole decrease in ketoconazole exposure. Nonetheless, re-acidification strategies to increase drug absorption in hypochlorhydric conditions seem to be a viable strategy. However, in a study with atazanavir, Coca-Cola® did not markedly reverse the decreased absorption due to omeprazole dosing (9). In order to sufficiently influence gastric pH in such a way as to mitigate reduced drug absorption, a large quantity of an acidic beverage would need to be given over a short period of time to facilitate dissolution of an oral drug.

Though it may seem viable, this method is flawed by the lack of consistency in the ability to provide ample gastric re-acidification under hypochlorhydric conditions. Additionally, the impact on the absorption of these weakly basic drugs may be limited as the pH of Coca-Cola® is only 2.5, which, for some drugs, may not contain enough acid to effectively mitigate this interaction. Moreover, repeated oral ingestion of a large volume of an acidic beverage is potentially harmful to oral and dental health (i.e. dental caries), and is likely not clinically acceptable in patients with symptoms of gastroesophageal reflux disease (GERD) due to the associated esophageal pain and discomfort of an acidic beverage. Therefore, we sought to develop a more reproducible and reliable strategy of gastric re-acidification under hypochlorhydric conditions that also has the potential to be more clinically acceptable.

Using a hydrochloric acid (HCl) supplement given in a solid oral dosage form such as a tablet or capsule would be more beneficial for this purpose, as the HCl would not directly come into contact with the mouth or esophagus. Additionally, the acidifying effect of the supplement would only activate once it reaches the stomach, where the salt can dissociate and produce free HCl. A paper published in 1991 characterized the effects of a solid oral dose of glutamic acid hydrochloride on gastric pH in healthy male volunteers receiving ranitidine. Glutamic acid hydrochloride lowered gastric pH to less than pH 2 within 15 minutes and remained under pH 3 for 45 minutes (10). While glutamic acid hydrochloride is no longer commercially available, a comparable salt, betaine hydrochloride (BHCl), has been more recently used as a gastric acid supplement and is available over the counter as a nutraceutical. Betaine is a naturally occurring substance that can be found in a variety of foods including beets, spinach, and whole wheat foods. Although BHCl has been used to supplement gastric acid, the time course and potency of this effect has not been thoroughly investigated in humans. Therefore, this pilot study aimed to characterize the ability of BHCl to reduce gastric pH under the influence of a proton-pump inhibitor (PPI), rabeprazole (Aciphex®) in healthy volunteers.

METHODS

Subject Enrollment and Study Design

Six healthy volunteers (4 male, 2 female) with ages between 25 and 57 years were enrolled in this single period, single treatment study (National Clinical Trials ID: #NCT01237353). Volunteers were non-smokers and had a mean (±SD) body mass index (BMI) of 25.2 (±3.8) kg/m^2. After providing written informed consent, all subjects underwent a screening visit to determine eligibility to participate in the study. The screening visit consisted

of a physical examination, medical history review, and measurement of baseline gastric pH using the Heidelberg pH Diagnostic System (Heidelberg Medical, Inc., Mineral Bluff, GA). This radio-telemetry system utilizes a small Heidelberg capsule that is tethered to a thin, pre-measured surgical string and given to subjects to swallow. Gastric pH measurements are then wirelessly transmitted from the capsule to a designated computer, which records pH data at 1-second intervals. Enrolled subjects did not have hypo- or achlorhydria (i.e. fasting pH was < 2), nor did they possess any history of gastrointestinal diseases. This study was approved by the Committee on Human Research of the University of California, San Francisco and registered on the US National Institutes of Health Clinical Trials Database (NCT01237353; https://clinicaltrials.gov/ct2/show/NCT01237353)

Data Analysis

Gastric pH data was recorded by the Heidelberg pH Diagnostic System over 1-second intervals. From this, pH data at 1-minute intervals were then reported and used for subsequent analyses, as it had been previously shown that pH data sampled at 1-minute intervals can accurately depict the pH-time profile (10). To evaluate the potency of BHCl, the lowest pH during a 15- and 30-minute interval after BHCl administration was subtracted from the median pH value over a 15- and 30-minute interval before BHCl administration, respectively.

The onset of effect of BHCl was determined by the time necessary for gastric pH to fall to less than pH 3, while the duration of effect of BHCl was measured by calculating the rebound time necessary for gastric pH to rise above pH 3 and pH 4, relative to BHCl administration. As a secondary method to evaluate BHCl efficacy, area under the pH versus time curves (AUC_{pH}) were calculated using a modification of the Trapezoidal Rule, beginning with BHCl

administration until the end of the study. To calculate the AUC_{pH} below pH 3 or pH 4, the difference between the observed pH and pH 3 or pH 4 was multiplied by the time interval (1 minute) for each time point. At any given time, if the observed pH exceeded the pH 3 or pH 4, those AUCs were reported as zero.

Statistical Analyses

The sample size was calculated based on a previously reported change in gastric pH of -4.6 ± 1.0 pH units after 1360 mg (7.6 mmol H^+) of glutamic acid HCl was administered to healthy volunteers treated with ranitidine (10). With a two-sided α=0.05 and 90% power, 5 subjects would be necessary to detect a 2 unit difference in gastric pH before and after the administration of 1500 mg (9.7 mmol H^+) of betaine HCl. Thus, a sample size of 6 was chosen to account for patient compliance and improve the estimations of our study endpoints.
All statistical tests were performed using GraphPad Prism 5 for Windows Version 5.02 (La Jolla, CA). Differences in gastric pH values before and after BHCl administration were tested for statistical significance using a Student's Paired, Two-tailed *t*-test, whereas AUC_{pH} correlations were tested for statistical significance using a non-parametric Spearman Rank Correlation test. Statistical significance was achieved with $P < 0.05$.

RESULTS

Gastric pH Monitoring

Representative gastric pH plots from two subjects during the fifth study day can be found in **Figure 2.1**.

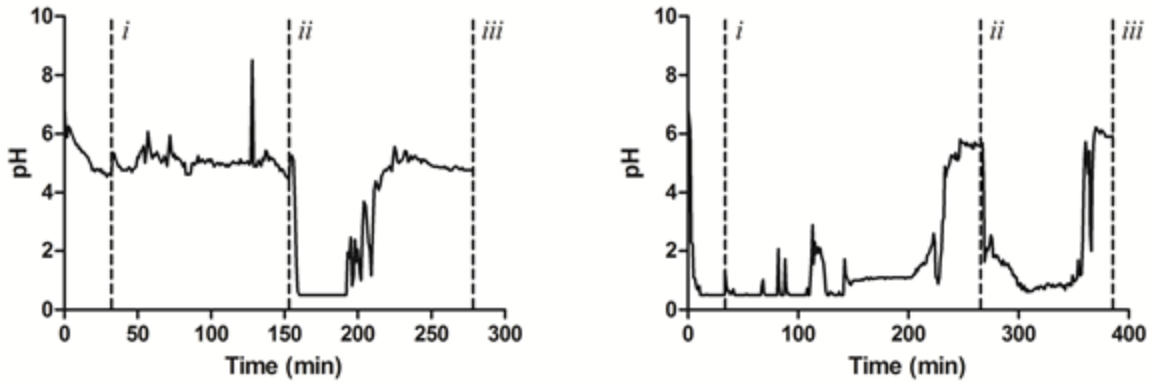

Figure 2.1 Sample gastric pH data of two subjects captured by the Heidelberg pH Capsule. Gastric pH measurements at 1-minute intervals were plotted versus time to produce the following curves. Vertical dashed lines (- - -) mark the following study events: (*i*) administration of 20 mg oral rabeprazole with 90 mL of water, (*ii*) administration of 1500 mg oral BHCl with 250 mL of water, and (*iii*) study end. The left curve represents a "best-case scenario," where a subject began the study day with a gastric pH > 4 after pre-treatment with rabeprazole for 4 days. In contrast, the right curve represents a "worst-case scenario," where a subject began the study with pH < 4. In these instances, BHCl was not administered until gastric pH remained above 4 for at least 15 minutes.

Though all subjects were pre-treated with multiple doses of rabeprazole, fasting gastric pH at the beginning of the fifth study day was not always above 4. This may most likely be due to the nocturnal gastric acid breakthrough that occurs overnight, even after twice-daily dosing of a PPI (11). It is interesting to note that those subjects who had a fasting gastric pH > 4 at the beginning of the study day took their doses with a meal, which supports the hypothesis that PPIs only inhibit active proton pumps in the stomach (11).

Potency of Betaine HCl Re-acidification

The average (±SD) gastric pH during the 15- and 30-minute interval just before BHCl administration was found to be 5.1 (±0.5) and 5.2 (±0.5), respectively, confirming that the rabeprazole dosing regimen chosen for the study was sufficient to induce hypochlorhydria in each subject.

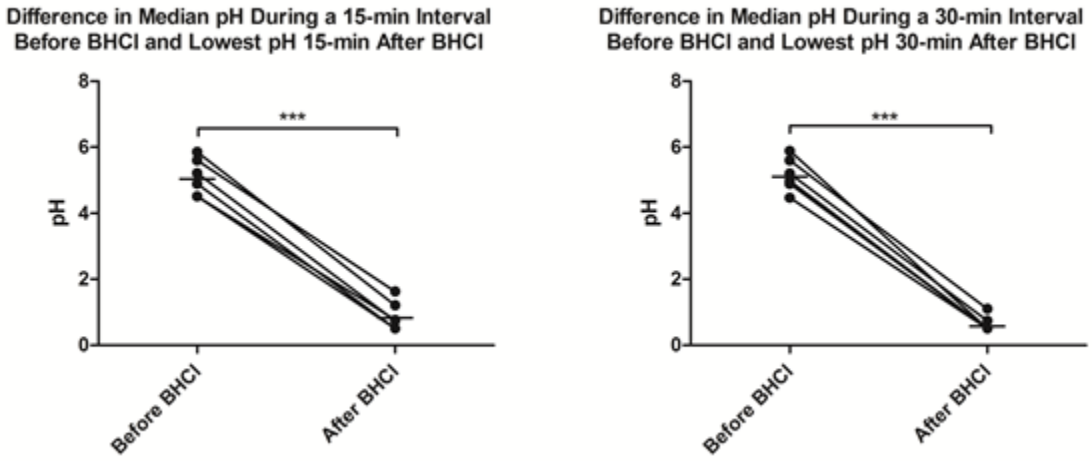

Figure 2.2 Potency of BHCl administration in healthy volunteers with rabeprazole-induced hypochlorhydria. Gastric pH was compared at equal time intervals (15 and 30 minutes) before and after BHCl administration. In both time intervals, gastric pH ranged from 4.5-5.9 before BHCl, with a mean pH of 5.1 (±0.5) and 5.2 (±0.5) for the 15- and 30-minute intervals, respectively. After BHCl administration, the mean gastric pH dropped to 0. 9 (±0.4) and 0.6 (±0.2), ranging between 0.5-1.6 and 0.5-1.1, for the 15- and 30-minute intervals, respectively. Means of 6 subjects are represented by horizontal bars.
(***P <0.001)

As seen in **Figure 2.2**, gastric pH was significantly reduced (P <0.001) after the administration of BHCl, with the lowest pH values over a 15- and 30-minute interval of 0.9 (±0.4) and 0.6 (±0.2), respectively. This corresponds to a mean change in pH (ΔpH) of 4.2 (±0.3) and 4.6 (±0.5) units for the 15- and 30-minute intervals, respectively.

Time Course of Betaine HCl

Table 2.1 summarizes the time course of BHCl for each subject. The onset of effect of BHCl was rapid, taking only 6.27 (±4.29) minutes to reach a pH < 3 when 1500 mg BHCl was given orally with 250 mL of water. The duration of BHCl re-acidification was also temporary, with rebound times to pH 3 and pH 4 averaging 73 (±33) and 77 (±30) minutes, respectively.

Table 2.1 Onset and duration measures of gastric re-acidification using BHCl after rabeprazole-induced hypochlorhydria.

Subject	Time to pH < 3 (Post-BHCl, min)	Rebound Time to pH > 3 (min)	Rebound Time to pH > 4 (min)
P-001	2.13	29	42
P-002	12.6	83	83
P-003	4.05	46	53
P-004	1.83	90	90
P-005	8.83	121	127
P-006	8.23	66	66
Mean (±SD)	6.27 (±4.29)	73 (±33)	77 (±30)

Onset of effect is characterized by the time to pH < 3, while the duration of effect is characterized by the rebound times to pH > 3 and pH > 4.

AUC_{pH} Below pH 3 and pH 4

The individual AUC_{pH} values for each patient can be found below in **Table 2.2**. When comparing AUC_{pH} below pH 3 or AUC_{pH} below pH 4 with the ΔpH after BHCl administration,

no correlations were found (P=0.66 and P=0.42, respectively). However, as expected, correlations were found between the AUC_{pH} below pH 3 and rebound time to pH > 3 (r=0.9; *P*=0.03) and AUC_{pH} below pH 4 and rebound time to pH > 4 (r=1.0; P=0.003).

Table 2.2 Individual AUC_{pH} values calculated below thresholds of pH 3 and pH 4.

Subject	AUC Below pH < 3 (ΔpH*min)	AUC Below pH < 4 (ΔpH*min)
P-001	70.1	108
P-002	178	259
P-003	104	156
P-004	169	261
P-005	281	409
P-006	91.0	157
Mean (±SD)	149 (±78)	225 (±109)
Spearman-r Coefficient[a]	0.89	1.0

[a]Spearman-r coefficients are reported for correlations between AUC_{pH} measures and their respective rebound times to pH > 3 and pH > 4.

Serum Gastrin Measurements

Serum gastrin levels measured during the study day are depicted in **Figure 2.3**. No significant relationships were found between gastrin levels and gastric pH measures.

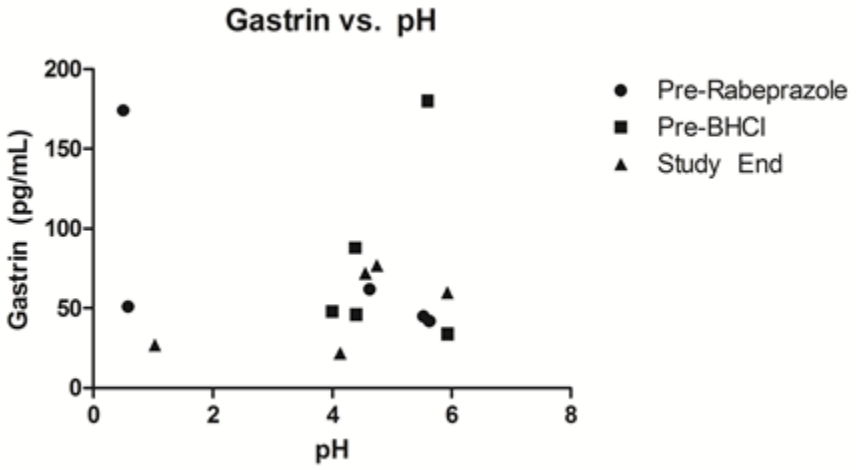

Figure 2.3 Serum gastrin levels at major study events and the corresponding observed gastric pH. Serum gastrin levels (pg/mL) were measured three-times on each study day: before rabeprazole dosing, before BHCl dosing, and at the end of the study day. No significant relationships were observed between serum gastrin and gastric pH with respect to the artificial changes in pH due to rabeprazole and BHCl.

Safety

All 6 subjects who were enrolled completed the study. No significant adverse events were observed. Moreover, no gastrointestinal side effects as a result of BHCl administration were observed.

DISCUSSION

In this pilot study, we demonstrated that 1500 mg of BHCl significantly (P <0.001) and safely reduced gastric pH in healthy subjects with pharmacologically-induced hypochlorhydria by over 4 pH units (**Figure 2.2**), lowering gastric pH from above pH 5 to below pH 1 for more than an hour. These findings support the further investigation of BHCl as a solid oral dosage

form of HCl that can potentially aid in the absorption of orally administered weakly basic drugs with pH-dependent solubility given under hypochlorhydric conditions.

Hypochlorhydria (or achlorhydria) is defined as a lack (or absence) of acid in the gastric fluid, and can be caused by medical conditions such as *Helicobacter pylori* infection (12) or autoimmune metaplastic atrophic gastritis (13). Hypochlorhydria can also be induced through the repeated administration of acid-reducing agents, such as proton-pump inhibitors (PPIs) or H_2-receptor antagonists (H2RAs), commonly used to manage symptoms of gastroesophageal reflux disesase or peptic ulcer disease. Individuals on daily drug regimens of acid-reducing agents therefore will have high gastric pH. From a pharmacologic perspective, gastric acid is important for the dissolution and solubilization of many solid oral dosage form medications and therefore is critical in oral drug absorption. Thus, conditions in which gastric acid levels are lowered or suppressed can lead to drug-drug interactions (DDIs) resulting in altered systemic concentrations and drug exposures. For example, for weakly basic drugs that exhibit pH-dependent solubility over a pH range of 1 to 4, the fraction of the dose available to the body for absorption will be severely reduced when gastric pH is > 4, limiting drug absorption and systemic exposure during acid-reducing agent therapy. In this scenario, temporary gastric re-acidification during drug administration may be helpful.

A gastric pH $\leq$ 2 was thought to be sufficiently acidic to improve the solubility of weakly basic drugs with pH-dependent solubility. Therefore, a 1500 mg dose of BHCl (2-750 mg tablets) was chosen as it provides the equivalent of 9.7 mmol of hydrogen ions (H^+), which equates to pH 1.41 in 250 mL of water. Though 1-750 mg tablet will produce over 4.8 mmol of H^+ and a pH of 1.71, two tablets were used to guarantee a more consistent gastric re-acidification across patients. An acidic beverage, such as Coca-Cola® for example, was reported to have a pH

of 2.5 (1). If a drug was administered with 250 mL of the beverage, this would only provide 0.79 mmol of H^+, which is much less than a single 750 mg tablet of BHCl that could provide over 4.8 mmol of H^+. BHCl provides an additional benefit over acidic beverages as the solid oral dosage form supplies acid directly to the stomach with no contact to the esophageal walls, minimizing potential patient discomfort and poor oral hygiene associated with repeated dosing. Furthermore, betaine is a safe and important human nutrient obtained from the diet from a variety of foods. Intake of betaine from foods is estimated to be 200-400 mg/day (14), and betaine doses of 6 to 20 grams per day are used safely to therapeutically treat homocystinuria (15).

Drug absorption can only be improved for weakly basic compounds if there is adequate exposure to a more acidic environment. If a drug was administered following BHCl dosing and the duration of re-acidification was not adequate, gastric pH would recover too quickly and there would be a minimal effect on the drug's dissolution and solubility. However, BHCl should provide ample time for gastric re-acidification (time of gastric pH < 4 ranged from 42 to 127 minutes), considering that for "rapidly dissolving" drugs, 85% of the labeled amount of drug is dissolved within 30 minutes (16).

The onset of the re-acidification was also favorable, with a mean onset of 6.3 minutes, ranging between 1.8 and 12 minutes (**Table 2.1**). This rapid onset of gastric re-acidification is important from a practical standpoint, as this minimizes the time between the dosing of BHCl and a theoretical victim drug. Having a short activation time also allows this strategy to be more applicable in a real-life patient scenario, where co-administration of BHCl and a victim drug would be more commonplace. Nonetheless, while this may help improve overall drug absorption, we do recognize the potential risks of having exposure to high gastric acidity in

actual patients who are on an acid-reducing agent for gastrointestinal disorders. As a proof-of-concept study, only one dose of BHCl was chosen and only healthy volunteers were enrolled. Thus, further studies are warranted to investigate the dose-response of BHCl on the potency and duration of gastric re-acidification and the tolerability of BHCl in patients on acid-reducing agents for GERD or other gastrointestinal disorders.

While ΔpH and rebound times to pH > 3 and > 4 were used as the primary markers of BHCl activity, the AUC_{pH}'s below pH 3 and pH 4 have also shown to have some value. Significant correlations were found between the AUC_{pH} below pH 3 and pH 4 and their respective rebound times, making it a secondary measure of the duration of gastric re-acidification as opposed to the potency. As each subject received the same dose of BHCl, the observed ΔpHs did not vary significantly, with coefficients of variation less than 10%. Although the pH-time data can directly provide an estimate of the length of the re-acidification period, the method can be flawed if the data are significantly affected by fluctuations in the pH above and below a given threshold. Using the AUC_{pH} can account for these fluctuations because only the parts of pH-time curves that are actually spent below pH 3 and pH 4 are integrated into the AUC_{pH} calculations, thereby limiting the effect that the variability in pH measurements may have.

In addition to the potency and duration parameters, serum gastrin was examined for its ability to be a predictor of gastric re-acidification following BHCl administration. Gastrin is a hormone produced by antral G cells that is a potent inducer of gastric acid secretion (17) and can be affected via negative feedback in the presence of gastric acid, where its release is inhibited (18). We found no significant relationships between serum gastrin levels and gastric pH (**Figure**

2.3), indicating that while the hormone is actively involved in the regulation of gastric acid, it is not predictive of the presence of gastric acid from BHCl administration.

CONCLUSIONS

The results of this pilot study have shown that BHCl can be used as an effective method to rapidly and temporarily lower gastric pH in healthy volunteers with drug-induced hypochlorhydria. This strategy has several advantages over previous methods of gastric re-acidification. It utilizes a commercially available, oral, natural supplement that can be purchased over the counter, making it easy for potential patients to obtain and use, thereby avoiding the harm and discomfort that can arise as a result of the ingestion of a large quantity of acidic fluid. BHCl has a rapid onset of effect, which allows convenient co-administration with a potential victim drug a possible outcome. Additionally, the duration of gastric re-acidification is temporary, yet sufficient, giving ample time for the dissolution of victim drugs that may be formulated as an immediate release dosage form. Lastly, it is possible that the degree of gastric re-acidification may be tailored to specific patients by altering the administered dose of BHCl, though the dose-dependencies of these effects still require further evaluation.

For weakly basic drugs that are administered orally under drug-induced hypochlorhydria, co-administration of BHCl may have a positive impact on the pharmacokinetics of the compound. Small-molecule, molecularly targeted anti-cancer agents are a class of drugs that have pH-dependent solubility and can be negatively affected by the effects of acid-reducing agents (19). Moreover, many cancer patients on a drug regimen consisting of these anti-cancer medications are also on some type of acid-reducing agent to mitigate adverse gastrointestinal side effects as a result of their disease or treatment (20). Furthermore, the potential for DDIs is

heightened given the high availability of acid-reducing agents over the counter, combined with the frequency of the practice of poly-pharmacy in any given patient population. Therefore, we hypothesize that the use of BHCl can be a viable strategy to improve the reduced drug absorption of these anti-cancer agents when given under drug-induced hypochlorhydria.

ACKNOWLEDGEMENTS

The authors would like to acknowledge the staff and nurses of the UCSF-CCRC for their assistance in this study. The UCSF-CCRC is supported by an NIH/NCRR Grant (Number UL1 RR024131). This study was supported by a grant from Genentech, Inc., and M. R. Yago was supported in part by NIH Training Grant T32 GM007175.

REFERENCES

1. Chin TW, Loeb M, Fong IW. Effects of an acidic beverage (Coca-Cola) on absorption of ketoconazole. Antimicrob Agents Chemother. 1995;39:1671-5.
2. Yin OQ, Gallagher N, Fischer D, Demirhan E, Zhou W, Golor G, et al. Effect of the proton pump inhibitor esomeprazole on the oral absorption and pharmacokinetics of nilotinib. J Clin Pharmacol. 2010;50:960-7.
3. Eley T, Luo FR, Agrawal S, Sanil A, Manning J, Li T, et al. Phase I study of the effect of gastric acid pH modulators on the bioavailability of oral dasatinib in healthy subjects. J Clin Pharmacol. 2009;49:700-9.
4. Kis O, Zastre JA, Ramaswamy M, Bendayan R. pH dependence of organic anion-transporting polypeptide 2B1 in Caco-2 cells: potential role in antiretroviral drug oral bioavailability and drug-drug interactions. J Pharmacol Exp Ther. 2010;334:1009-22.
5. Zhu L, Persson A, Mahnke L, Eley T, Li T, Xu X, et al. Effect of low-dose omeprazole (20 mg daily) on the pharmacokinetics of multiple-dose atazanavir with ritonavir in healthy subjects. J Clin Pharmacol. 2011;51:368-77.
6. Itraconazole (Package Insert). Laurelton, New York: Eon Labs, Inc.; **2012**.
7. Jaruratanasirikul S, Sriwiriyajan S. Effect of omeprazole on the pharmacokinetics of itraconazole. Eur J Clin Pharmacol. 1998;54:159-61.
8. Blum RA, D'Andrea DT, Florentino BM, Wilton JH, Hilligoss DM, Gardner MJ, et al. Increased gastric pH and the bioavailability of fluconazole and ketoconazole. Ann Intern Med. 1991;114:755-7.
9. Agarwala S, Gray K, Eley T, Wang Y, Hughes E, Grasela D. Pharmacokinetic interaction between atazanavir and omeprazole in healthy subjects. 3rd IAS Conference on HIV Pathogenesis and Treatment; Rio de Janiero, Brazil. July 24-27, 2005.

10. Knapp MJ, Berardi RR, Dressman JB, Rider JM, Carver PL. Modification of gastric pH with oral glutamic acid hydrochloride. Clin Pharm. 1991;10:866-9.
11. Peghini PL, Katz PO, Bracy NA, Castell DO. Nocturnal recovery of gastric acid secretion with twice-daily dosing of proton pump inhibitors. Am J Gastroenterol. 1998;93:763-7.
12. El-Omar EM, Oien K, El-Nujumi A, Gillen D, Wirz A, Dahill S, et al. Helicobacter pylori infection and chronic gastric acid hyposecretion. Gastroenterology. 1997;113:15-24.
13. Gastritis and Peptic Ulcer Disease. In The Merck Manual for Health Care Professionals, 19th ed (online). Whitehouse Station, NJ: Merck Sharp & Dohme Corp.; 2013.
14. Fischer LM, Scearce JA, Mar MH, Patel JR, Blanchard RT, Macintosh BA, et al. Ad libitum choline intake in healthy individuals meets or exceeds the proposed adequate intake level. J Nutr. 2005;135:826-9.
15. Betaine Anhydrous for Oral Solution (Cystadane®, Package Insert). Franklin, TN: Rare Disease Therapeutics, Inc.
16. The US Food and Drug Administration. Guidance For Industry - Waiver of In Vitro Bioavailability and Bioequivalence Studies for Immediate-Release Solid Oral Dosage Forms Based on a Biopharmacetics Classification System. 2000.
17. Hoogerwerf WA, Pasricha, P. J., editor. Chapter 36. Pharmacotherapy of Gastric Acidity, Peptic Ulcers, and Gastroesophageal Reflux Disease. New York: McGraw-Hill; 2006.
18. Walsh JH, Richardson CT, Fordtran JS. pH dependence of acid secretion and gastrin release in normal and ulcer subjects. J Clin Invest. 1975;55:462-8.
19. Budha NR, Frymoyer A, Smelick GS, Jin JY, Yago MR, Dresser MJ, et al. Drug absorption interactions between oral targeted anticancer agents and PPIs: is pH-

dependent solubility the Achilles heel of targeted therapy? Clin Pharmacol Ther. 2012;92:203-13.

20. Smelick GS, Heffron TP, Chu L, Dean B, West DA, Duvall SL, et al. Prevalence of acid-reducing agents (ARA) in cancer populations and ARA drug-drug interaction potential for molecular targeted agents in clinical development. Mol Pharm. 2013;10:4055-62.

CHAPTER 3. THE USE OF BETAINE HCL TO ENHANCE DASATINIB ABSORPTION IN HEALTHY VOLUNTEERS WITH RABEPRAZOLE-INDUCED HYPOCHLORHYDRIA[1]

ABSTRACT

Many orally administered, small-molecule, targeted anti-cancer drugs, such as dasatinib, exhibit pH-dependent solubility and reduced drug exposure when given with acid-reducing agents. We previously demonstrated that betaine hydrochloride (BHCl) can transiently re-acidify gastric pH in healthy volunteers with drug-induced hypochlorhydria. In this randomized, single-dose, three-way crossover study, healthy volunteers received dasatinib (100mg) alone, after pretreatment with rabeprazole, and with 1500mg BHCl after rabeprazole pretreatment, to determine if BHCl can enhance dasatinib absorption in hypochlorhydric conditions. Rabeprazole (20mg b.i.d.) significantly reduced dasatinib C_{max} and $AUC_{0-\infty}$ by 94% and 83%, respectively. However, co-administration of BHCl significantly increased dasatinib C_{max} and $AUC_{0-\infty}$ by 15- and 6.7-fold, restoring them to 90% and 116%, respectively, of the control (dasatinib alone). Therefore, BHCl reversed the impact of hypochlorhydria on dasatinib drug exposure and may be an effective strategy to mitigate potential drug-drug interactions for drugs that exhibit pH-dependent solubility and are administered orally under hypochlorhydric conditions.

[1]Modified from publication: Yago MR, Frymoyer A, Benet LZ, Smelick GS, Frassetto LA, Ding X, et al. The use of betaine HCl to enhance dasatinib absorption in healthy volunteers with rabeprazole-induced hypochlorhydria. AAPS J. 2014; 16:1358-65.

INTRODUCTION

Drug-drug interactions due to changes in gastric pH typically result in alterations of drug solubility, which can subsequently impact drug absorption and exposure. These interactions can have clinically significant consequences, as increased or reduced systemic concentrations can result in drug toxicity or decreased therapeutic efficacy. For orally administered drugs that exhibit a pH-dependent solubility over the range of pH 1-4, the likelihood for an interaction of this nature to occur is higher, as normal fasting gastric pH ranges between pH 1-3 (1) while gastric pH becomes elevated to ≥ 4 during administration of acid-reducing agents (ARAs) such as proton-pump inhibitors (PPIs) or H_2-receptor antagonists (H2RAs). ARAs are commonly used to manage symptoms of gastroesophageal reflux disease (GERD) or peptic ulcer disease. In the United States, it was estimated that PPIs were prescribed for greater than 50% of digestive diseases, which resulted in an estimated health-care cost of more than $11 billion (2), and does not include ARAs purchased over-the-counter (OTC). Therefore, the wide usage of ARAs together with the increasing frequency of polypharmacy (3) increases the likelihood that drug-drug interactions associated with a drug-induced increase in gastric pH may occur.

For many orally administered, weakly basic compounds with pH-dependent solubility, co-administration with ARAs has been shown to lower drug solubility at the time of their administration, thereby reducing systemic concentrations and drug exposure (4-6). Although the severity of this interaction can depend on the therapeutic window of the drug and on the degree to which drug solubility is pH-dependent, small molecule anti-cancer agents are at risk for having much lower oral bioavailability and subtherapeutic concentrations when co-administered with ARAs (7). The significance of the interaction between these anti-cancer agents and gastric pH is further emphasized by the finding that approximately 33% of patients receiving an anti-

cancer agent are also prescribed an ARA (8). As such, for a number of orally administered anti-cancer agents, it is advised to avoid concomitant administration with ARAs, due to potentially clinically significant reductions in drug exposure and therapeutic effect (9-13).

One such compound affected by this gastric pH interaction is dasatinib (Sprycel®), which is a tyrosine kinase inhibitor used in the treatment of chronic phase, Philadelphia Chromosome (Ph+)-positive chronic myeloid leukemia (CML) and imatinib-resistant/intolerant CML (9). Dasatinib is weakly basic in nature and exhibits a pH-dependent solubility, becoming practically insoluble in water above pH 6 (solubility <0.008 mg/mL) (9). In a study published in 2009, dasatinib area under the concentration versus time curve (AUC) and maximum plasma concentration (C_{max}) were reduced by approximately 60% when given following a single oral dose of famotidine (40 mg), an H2RA, administered 10 hours prior (5). Although it has been proposed to further separate the time the two drugs are administered as a way to possibly prevent this interaction, a dose timing strategy might not always be clinically feasible. In addition for more potent ARAs such as PPIs, where gastric acid inhibition is more potent and prolonged, a dose timing strategy would not work. Therefore, a transient gastric re-acidification at the time of drug dosing may aid in mitigating this gastric pH-drug-drug interaction.

Previously, oral acidic solutions (i.e. cola beverages) have been used in an attempt to raise the extent of drug absorption following administration of a weakly basic drug with an ARA (4, 14, 15). However, data from these studies suggest that this strategy may be inconsistent for various weakly basic drugs, as cola was unable to consistently reverse the reduced absorption caused by the ARA. Furthermore, the use of colas to improve drug absorption can be hampered by the harm that may result from a large volume of acidic fluid that may come into contact with the esophagus, as well as an increased risk of dental damage due to the formation of caries. For

this purpose, gastric re-acidification in the form of a solid oral dosage form may prove to have a higher utility.

Betaine hydrochloride (BHCl) is an OTC natural supplement that can be commonly found in digestive aids. As a solid oral dosage form, BHCl acidifies gastric fluid by dissociating into free betaine and hydrochloric acid, thus lowering gastric pH. We recently characterized the ability of BHCl to re-acidify gastric pH in healthy volunteers pre-treated with rabeprazole, a PPI, reporting that BHCl was able to safely, significantly, and transiently lower gastric pH under rabeprazole-induced hypochlorhydria. A 1500mg dose of BHCl resulted in a decrease in gastric pH on average from pH 5 to pH 1, with a gastric pH <3 achieved on average for 73 minutes (16). Therefore, BHCl co-administration may be a potential strategy to mitigate drug-drug interactions with gastric pH. The goal of this randomized, single-dose, three-treatment cross-over study reported here was to investigate whether BHCl can mitigate the reduced dasatinib absorption observed in healthy volunteers with rabeprazole-induced hypochlorhydria.

METHODS

Subjects

Ten self-declared nonsmoking subjects (9 male, 1 female) between 23–59 years of age, with body mass indexes ranging from 21.6–29.1, and taking no concomitant medications were enrolled in this three-treatment crossover study. After providing written informed consent, subjects underwent a screening visit, which occurred at least 1 week prior to the start of the study, consisting of a medical history review, physical examination, electrocardiogram, and standard clinical blood and urine laboratory tests, to determine eligibility to participate in the study. Screening visits also included baseline gastric pH measurements through the use of the

Heidelberg pH Diagnostic System (Heidelberg Medical Inc., Mineral Bluff, GA), to confirm normochlorhydria (fasting gastric pH < 4), as previously described (16). All subjects enrolled in this study did not have hypo- or achlorhydria, nor did they have any prior reported history of gastrointestinal diseases. A summary of patient enrolled patient demographics can be found in **Table 3.1**.

This study was approved by the Committee on Human Research of the University of California, San Francisco and registered on the US National Institutes of Health Clinical Trials Database (NCT01398046; http://clinicaltrials.gov/ct2/show/NCT01398046).

Table 3.1 Summary of enrolled subject demographics.

Total N	**10**
Male	9
Female	1
Race/Ethnicity	
Caucasian	6
Asian	3
African-American	1
Age (years)	
Mean ± SD	38 ± 11
Range	23—59
Baseline Gastric pH	
Median (Range)	0.6
Range	0.5—1.8

Subjects had no prior history of gastrointestinal diseases as determined by a medical history review. Baseline gastric pH measurements were taken during the initial screening visit, and represents the median gastric pH observed in a 15-minute interval after placement of the Heidelberg Capsule.

Study Design

This open-label, three-treatment, randomized clinical pharmacokinetic crossover study was conducted at the Clinical & Translational Science Institute's Clinical Research Center (CCRC) located at the University of California, San Francisco. All enrolled subjects received

the first treatment (Treatment A), which was a single 100 mg dose of dasatinib (Bristol-Myers Squibb, New York City, NY) given orally with 250 mL of water. Subjects were then block-randomized using a random number generator (N = 6 subjects per block) for the order in which they would receive treatments B and C. Both treatments began with a pretreatment phase during which subjects self-administered 20 mg of rabeprazole (Eisai Co., Ltd., Woodcliff Lake, NJ) with food, twice daily for three days. An additional 20 mg dose was given on the morning of the fourth study day, and once gastric pH remained above pH ≥4 for at least 15 minutes, subjects then received either a single 100 mg dose of dasatinib with 250 mL of water (Treatment B), or 1500 mg of betaine HCl, followed by 100 mg dose of dasatinib five minutes later with a total of 250 mL of water (Treatment C). Heidelberg pH capsules were administered to subjects on the morning of each study day, and gastric pH measurements were taken until three hours post dasatinib dosing. All subjects were fasted from midnight the night prior and remained fasted until gastric pH measurements were completed. Subjects were also required to record dates and times of all self-administered rabeprazole doses in addition to any adverse events experienced, in a verified medication diary. All dasatinib doses were separated by at least a seven-day washout period, and subjects completed all three treatments by the end of study.

Venous blood samples were drawn at the following times with respect to dasatinib dosing: pre-AM rabeprazole dose (Treatments B and C only), 0, 0.5, 1, 1.5, 2, 3, 4, 6, 8, 12, and 22 hours. Blood samples were centrifuged within 30 minutes at 4°C. Plasma was then separated and stored in aliquots at -80°C until bioanalysis. Plasma concentrations of dasatinib and rabeprazole were measured using a validated LC-MS/MS method (Covance, Inc., Madison, WI), as described below.

Outcome Measures

The primary outcome measures for this study included plasma dasatinib C_{max} and AUCs ($AUC_{0\text{-}22}$, $AUC_{0\text{-}\infty}$) for each treatment period. Dasatinib T_{max}, $t_{1/2}$, and oral clearance (CL/F) for all treatment arms were included as secondary outcomes for this study.

Pharmacokinetic Analyses

Dasatinib and rabeprazole pharmacokinetic parameters for each treatment period were estimated from measured plasma concentrations using noncompartmental analyses in Phoenix Winnonlin 5 (Pharsight®, Sunnvale, CA). C_{max} and T_{max} were estimated from the observed data. The terminal rate constant (λ_z) was calculated using a linear regression of the terminal phase of the log-linear concentration curve, and the terminal half-life was calculated using $\ln 2/\lambda_z$. Dasatinib and rabeprazole AUCs were calculated using the logarithmic-linear trapezoidal method, and extrapolated to infinity by dividing the last measured concentration by λ_z. Oral dasatinib and rabeprazole clearances (CL/F) were obtained by dividing the dose by $AUC_{0\text{-}\infty}$.

Statistical Analyses

Based on a 60% reduction in dasatinib AUC when administered in healthy volunteers pretreated with famotidine (5), it was determined that 18 subjects would be necessary to show a 50% increase in dasatinib AUC when co-administered with betaine HCl in healthy volunteers pre-treated with rabeprazole, with greater than 80% power and a two-sided α of 0.05, but subject number was decresased based on an interim analysis described below.

A repeated measures analysis of variance (ANOVA) with the Tukey's test for multiple comparisons was used to determine statistical significance across all treatments for all dasatinib

pharmacokinetic parameters except T_{max} (C_{max}, AUC_{0-22}, $AUC_{0-\infty}$, CL/F, and $t_{1/2}$). Differences in dasatinib T_{max} values were tested for statistical significance using the Friedman test for multiple comparisons with $\alpha = 0.05$, and a Dunn's post-test for all-by-all comparisons. With the exception of T_{max}, results of all pharmacokinetic parameters are reported as means ± SD. Results for T_{max} are reported as medians, with ranges in parentheses. A two-tailed, paired *t*-test with $\alpha = 0.05$ was used to test for statistically significant differences in rabeprazole pharmacokinetic parameters.

Interim Analyses

An interim analysis was performed after the first block of subjects completed all treatments of the study to assess if the study should be terminated due to a lack of effect and further risk of administering an anti-cancer agent to healthy volunteers. Surprisingly, results of this interim analysis showed statistically significant differences in all primary outcome measures between treatments B and C, with $P < 0.05$. As such, it was determined that a modified sample size of 10 subjects would be sufficient to complete the study, without unnecessary exposure to dasatinib in other healthy volunteers.

Quantitative Determination of Dasatinib and Rabeprazole

Qualified high performance liquid chromatography tandem mass spectrometry (LC-MS/MS) methods were used for the analysis of dasatinib and rabeprazole in human plasma. Dasatinib plasma samples were cleaned using supported liquid extraction before analysis. Fifty µL of dasatinib plasma samples, calibration standards or quality control (QC) samples were added to a 96-well plate followed by the addition of 50 µL of internal standard (d_8-dasatinib, 200

ng/mL) and 100 µL of water. Following vortexing and centrifugation at 1640 x g for a minute, 200 µL of each sample mixture was loaded onto an Isolute SLE+ plate (Biotage, Charlotte, NC). After equilibrating for 5 minutes, samples were eluted with 800 µL of tert-butyl methyl ether, dried under nitrogen and reconstituted in a methanol:water mixture (1:2, v/v) with 0.1% formic acid. For rabeprazole, 25 µL of plasma samples, calibration standards or quality control (QC) samples were added to a 96-well plate followed by the addition of 25 µL of internal standard (d_3-rabeprazole, 200 ng/mL). Proteins were precipitated with the addition of 200 µL of methanol. Following vortexing and centrifugation at 1640 x g for 5 minutes, 150 µL of each supernatant was mixed with 150 µL of water. Processed samples were then injected into the LC-MS/MS for analysis.

The LC-MS/MS system consisted of an LC-20AD and SIL-20AC Prominence HPLC system (Shimadzu, Columbia, MD) and an AB Sciex API 4000 mass spectrometer (AB Sciex, Foster City, CA) equipped with a turbo-ionspray source operating in the positive ionization mode. Separation was achieved using reverse-phase liquid chromatography with a 3 µm 50 x 2.1 mm Pursuit PFP Column (Varian, Palo Alto, CA) for dasatinib and 3 µm 50 x 2.1 mm BetaBasic C18 Column (Thermo, Waltham, MA) for rabeprazole. Gradient elution was used at a flow rate of 0.7 mL/min for dasatinib and 0.6 mL/min for rabeprazole, with a retention time of 1.3 minutes for both dasatinib and rabeprazole. Mobile phases consisted of (A) water and (B) methanol, each containing 0.1% formic acid. Quantitation was performed using multiple reaction monitoring (MRM) for the following mass transitions: m/z 488 to 401 for dasatinib, m/z 496 to 406 for d_8-dasatinib, m/z 360 to 242 for rabeprazole and m/z 363 to 245 for d_3-rabeprazole. Accuracy and precision (relative standard deviation) were within 75 % to 125 % (70% to 130% for LLOQ).

RESULTS

Gastric Re-acidification Using Betaine HCl

The time course and potency of BHCl on gastric pH in rabeprazole pre-treated subjects are summarized in **Table 3.2**.

Table 3.2 Time course and potency of gastric re-acidification using BHCl in healthy subjects with rabeprazole-induced hypochlorhydria.

Time Course of BHCl	**Mean ± SD (min)**		
Onset (Time to pH <3)	12 ± 21		
Rebound Time to pH >3	69 ± 77		
Potency of BHCl			
	pH before BHCl	**pH after BHCl**	**ΔpH**
Mean ± SD	4.1 ± 0.9	0.74 ± 0.54	3.4 ± 0.9
Range	2.8—5.2	0.50—3.6	0.61—4.7

Gastric pH data at 1-minute intervals from Treatment C were used to calculate the time course and potency of BHCl. The time course is described by the onset of effect (time to pH <3) and rebound time to pH >3, relative to BHCl administration, while the potency is described by the ΔpH calculated before and after BHCl administration.

The onset of effect of BHCl, measured as the time necessary to achieve gastric pH <3, was quick, averaging 12 minutes. Gastric pH was significantly lower after BHCl (ΔpH -3.4 ± 0.9; *P* <0.001). In addition, a return to a gastric pH >3 required an average of 69 minutes after BHCl administration, indicating that the gastric re-acidification period was temporary. All subjects achieved a gastric pH <3 for at least 26 minutes.

Dasatinib Pharmacokinetics

The mean plasma concentration-time curves of dasatinib for ten subjects following a 100 mg oral dose of dasatinib on each of the three treatment days are shown in **Figure 3.1**.

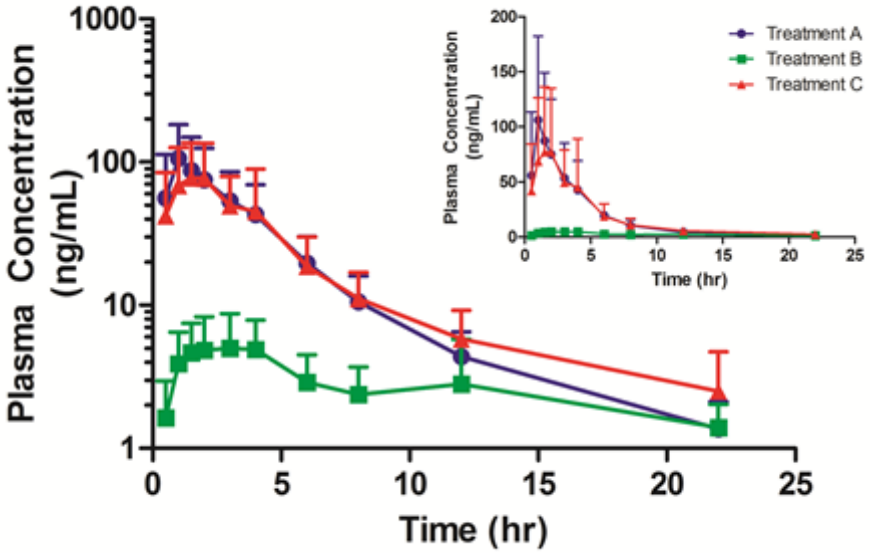

Figure 3.1 Effects of gastric pH modulators on plasma concentrations of dasatinib in healthy volunteers. A single-oral dose of 100 mg dasatinib was given on each study day either alone (Treatment A), after pretreatment with rabeprazole (Treatment B), or after pretreatment with rabeprazole followed by betaine HCL given 5 min prior to dasatinib (Treatment B)**.** Points represent the mean of ten subjects (error bars indicating the SD) plotted on a logarithmic scale, with the inset graphs plotted on a linear scale.

Dasatinib pharmacokinetics in Treatment A were comparable to those previously reported in healthy volunteers receiving the same dose (9). When subjects were pre-treated with rabeprazole prior to dasatinib dosing (Treatment B), significant reductions (P <0.001) in dasatinib C_{max}, $AUC_{0\text{-}22}$, and $AUC_{0\text{-}\infty}$ of 94%, 85%, and 83%, respectively, were observed relative to dasatinib alone (Treatment A; **Table 3.3**).

Table 3.3 Dasatinib pharmacokinetics in 10 healthy volunteers following a 100 mg oral dose given with and without gastric pH modulators.

				Geometric Mean Ratios (90% CI)		
Parameter	**DAS Alone (Treatment A)**	**DAS + RAB (Treatment B)**	**DAS + RAB + BHCl (Treatment C)**	**B–to–A**	**C–to–B**	**C–to–A**
C_{max} (ng/mL)	115 ± 68	6.87 ± 3.57 ***;†††	103 ± 58	0.0757 (0.0342—0.168)	14.0 (7.7—25.4)	1.05 (0.48—2.30)
$AUC_{0\text{-}22}$ (ng/mL*hr)	395 ± 196	57.9 ± 28.7 ***;†††	379 ± 161	0.165 (0.090—0.303)	6.66 (4.23—10.5)	1.10 (0.623—1.92)
$AUC_{0\text{-}\infty}$ (ng/mL*hr)	405 ± 200	70.5 ± 24.8 ***;†††	469 ± 233	0.217 (0.113—0.417)	5.57 (3.81—8.14)	1.21 (0.671—2.17)
T_{max} (hr)	1.0 (1.0−4.0)	2.0 (1.5−12)	2.0 (0.50−4.0)	**N/A**	**N/A**	**N/A**
CL/F (mL/min/kg)	107 ± 114	376 ± 127 ***;†††	67.8 ± 42.0	4.62 (2.41—8.85)	0.180 (0.123—0.264)	0.835 (0.470—1.48)
$t_{1/2}$ (hr)	4.43 ± 0.64	11.2 ± 7.2 ***;††	5.29 ± 1.04	2.10 (1.42—3.11)	0.553 (0.391—0.781)	1.16 (1.03—1.31)

DAS, dasatinib; RAB, rabeprazole; BHCl, betaine HCl; C_{max}, maximum plasma concentration; T_{max}, time to maximum plasma concentration; $t_{1/2}$, terminal half-life; AUC, area under the plasma concentration-time curve; CL/F, oral clearance. Statistical results for Treatment B versus A comparisons (***P <0.001; **P <0.01) and Treatment C versus B comparisons (†††P <0.001; ††P <0.01) are reported in each row of the Treatment B column.

No significant differences were observed for all pharmacokinetic parameters in Treatment C versus A comparisons, and in T_{max} across all treatments.

However, with the addition of BHCl in rabeprazole pre-treated subjects (Treatment C), dasatinib C_{max}, AUC_{0-22}, and $AUC_{0-\infty}$ were significantly increased relative to rabeprazole pretreatment alone by 15-, 6.5-, and 6.7-fold, respectively (P <0.001 for all comparisons). Co-administration of BHCl with dasatinib under hypochlorhydric conditions was able to restore dasatinib C_{max}, AUC_{0-22}, and $AUC_{0-\infty}$ to 90%, 96%, and 116% of their respective values on dasatinib alone "control" treatment days (Treatment A).

In addition to the changes observed in dasatinib C_{max}, AUC_{0-22}, and $AUC_{0-\infty}$, oral clearance (CL/F) and half-life ($t_{1/2}$) of dasatinib were also sensitive to changes in gastric pH. In subjects with rabeprazole-induced hypochlorhydria, CL/F and $t_{1/2}$ were increased by over 3.5- and 2.5-fold, respectively (P <0.001), when compared to dasatinib given alone. However, the co-administration of BHCl lowered dasatinib CL/F and $t_{1/2}$ by 82% and 53%, respectively, thereby reversing the effects of the elevated gastric pH caused by rabeprazole. Furthermore, no significant differences in dasatinib CL/F and $t_{1/2}$ were observed between subjects in Treatment C versus Treatment A.

No significant differences were observed in dasatinib T_{max} across all treatments.

Correlation of Dasatinib C_{max} and AUC Ratios with Gastric Acid Exposure

Gastric acid exposure ($AUC_{pH<3}$) was calculated as previously described (16) for Treatment C, as a secondary measure of BHCl efficacy. As shown in **Figure 3.2**, significant, positive correlations (P <0.05; Spearman r >0.70) were observed between $AUC_{pH<3}$ and the increases in dasatinib C_{max} and AUC when given with BHCl under rabeprazole-induced hypochlorhydria (Treatment C).

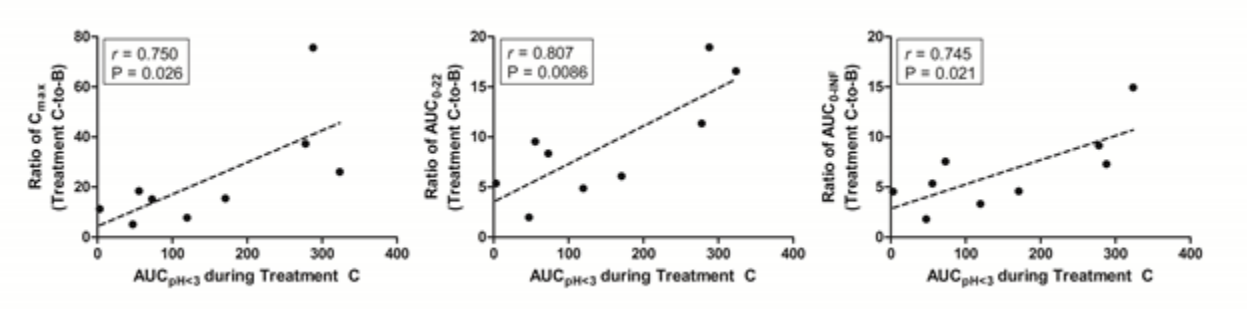

Figure 3.2 Relationship between gastric acid exposure ($AUC_{pH<3}$) during betaine HCl treatment and change in dasatinib C_{max} and AUC during rabeprazole-induced hypochlorhydria. The changes in dasatinib C_{max}, AUC_{0-22}, and $AUC_{0-\infty}$were calculated by taking the ratio of each parameter during Treatment C (Dasatinib + Rabeprazole + Betaine HCl) relative to Treatment B (Dasatinib + Rabeprazole). $AUC_{pH<3}$, a measure of overall gastric acid exposure, was calculated as previously described (16).

Rabeprazole Pharmacokinetics

Noncompartmental analyses of rabeprazole plasma concentrations for treatments B and C demonstrated that no difference in rabeprazole pharmacokinetics was observed with the addition of BHCl (**Table 3.4**).

Table 3.4 Rabeprazole pharmacokinetics in 10 healthy volunteers during rabeprazole pre-treatment study days.

Parameter	Treatment B	Treatment C	Geometric Mean Ratio (90% CI)
C_{max} (ng/mL)	538 ± 210	413 ± 150	0.755 (0.507—1.12)
AUC_{0-22} (ng/mL*hr)	968 ± 319	825 ± 312	0.843 (0.694—1.03)
$AUC_{0-\infty}$ (ng/mL*hr)	970 ± 320	830 ± 311	0.847 (0.699—1.03)
T_{max} (hr)	N/A	N/A	N/A
CL/F (mL/min/kg)	5.33 ± 1.88	6.34 ± 2.28	1.19 (0.978—1.44)
$t_{1/2}$ (hr)	2.57 ± 1.63	2.39 ± 1.75	0.863 (0.646—1.15)

C_{max}, maximum plasma concentration; T_{max}, time to maximum plasma concentration; $t_{1/2}$, terminal half-life; AUC, area under the plasma concentration-time curve; CL/F, oral clearance. No significant differences were observed in rabeprazole pharmacokinetics with the addition of BHCl. T_{max} values were unable to be estimated as plasma concentrations were measured at time points relative to dasatinib administration.

Safety

All 10 subjects enrolled received and completed all treatments. No adverse effects were reported due to dasatinib, rabeprazole or BHCl dosing. Additionally, no gastrointestinal side effects were reported due to rabeprazole or BHCl administration. Furthermore, subjects experienced no adverse events using the Heidelberg pH capsule during all phases of the study.

DISCUSSION

In this three-treatment, randomized, pharmacokinetic, crossover study, we demonstrated that a 1500 mg oral dose of BHCl was able to safely and significantly reverse the effect of rabeprazole-induced hypochlorhydria on the absorption of dasatinib in healthy volunteers. Dasatinib, a BCR-ABL tyrosine kinase inhibitor, is a weak base with pH-dependent solubility, and therefore is a prime substrate for drug-drug interactions due to changes in gastric pH. As many small-molecule, molecular-targeted anti-cancer agents share similar physicochemical

properties with dasatinib and display marked reductions in drug exposure when co-administered with ARAs (7), the addition of BHCl may prove to be a clinically valuable strategy to mitigate this significant drug-drug interaction by transiently re-acidifying gastric pH at the time of drug dosing.

Drug-drug interactions due to ARAs, particularly the PPIs, can involve significant reductions in drug absorption due to elevations in pH in the stomach and upper gastrointestinal regions (17), or increased drug exposure due to inhibition of the cytochrome P450 (CYP) metabolizing enzymes (18). Most PPIs are primarily metabolized in the liver by the CYP2C19 and CYP3A4 isoforms (19), and have the potential to cause drug-drug interactions with other drugs metabolized by the same CYPs. However, rabeprazole is unique as a PPI in that it is primarily metabolized by non-P450 mediated mechanisms (20). Therefore in the current study, metabolic interactions with dasatinib, which is primarily metabolized by CYP3A4 (21), were minimized and our ability to focus on the effects of gastric pH was enhanced. Although dasatinib CL/F was shown in our study to be sensitive to changes in gastric pH, these differences can be attributed to dasatinib bioavailability (F), which decreases as gastric pH increases due to the reduced dasatinib solubility at elevated gastric pH (pH >4). In a similar fashion, dasatinib $t_{1/2}$ was also sensitive to changes in gastric pH, as dasatinib elimination appears to become rate-limited by drug absorption during rabeprazole-pretreatment days.

The effects of elevated gastric pH on drug absorption of weakly basic drugs due to concomitant administration of ARAs have been widely studied, and it is well known that significant reductions in systemic concentrations and drug exposures are observed as a result (4-6). Interestingly, in the current study when subjects were administered dasatinib after rabeprazole pretreatment (Treatment B), the reductions in dasatinib C_{max} and AUC were far

greater than previously reported in studies using famotidine (5) or omeprazole (22), in which reductions of approximately 60% were seen. The more pronounced impact on PK seen in our study might be partially attributed to the use of twice daily dosing of rabeprazole as opposed to the once daily dosing of famotidine or omeprazole used in the prior studies. In addition, rabeprazole may provide a higher degree of acid secretion inhibition compared to other ARAs (23), resulting in greater alterations in gastric pH and a larger impact on dasatinib solubility and absorption. Importantly, our study design was optimized based on a previous methodology study (16) to achieve timely and maximum gastric pH alterations and included the utilization of continuous gastric pH measurements (i.e. Heidelberg capsules) on the study days. Therefore, we were able to confirm an elevated gastric pH in all patients at the time of dasatinib dosing.

To mitigate gastric pH interactions for weakly basic compounds such as dasatinib, strategies might include separating the times at which the ARAs are administered, increasing the dose of a potential victim drug, or transient gastric re-acidification. The separation of dosing times of a victim drug and weak ARAs, such as antacids, has been shown to mitigate the reduction in drug exposure caused by the elevated gastric pH (5). However, for H2RAs and PPIs, this may not be feasible as both drugs have the potential to inhibit acid secretion for a much longer time in a 24 hour period. Alternatively, increasing the dose of a victim drug is not likely to overcome this interaction, particularly if drug absorption is limited by its solubility. In this case, the maximum solubility of the drug would already have been achieved and further dose escalations would have no benefit. Lastly, transient gastric re-acidification is a strategy that artificially lowers gastric pH through the use of oral acidifying agents, such as acidic beverages or hydrochloric acid salts. However, as described above, the use of acidic beverages does not completely reverse the effects of hypochlorhydria and is limited by the pH of the solutions used,

the large volumes necessary to sufficiently acidify gastric pH, and the potential dental and esophageal damage that may result from chronic administration. As a solid, oral dosage form, BHCl can improve gastric re-acidification strategies due to the ease of administration and minimal direct exposure of acid to the mouth and esophagus.

The use of BHCl in this study proved to be a safe and successful way to mitigate the reduction in dasatinib absorption during rabeprazole-induced hypochlorhydria, nearly raising C_{max} and AUC to levels observed during treatment with dasatininb alone (i.e. under normochlorhydric conditions; Treatment A). This effect can be attributed to the large change in gastric pH (mean ΔpH -3.4) that was of rapid onset (mean time to pH <3 was 12 minutes) after a 1500 mg dose of BHCl. In addition, the time period of re-acidification was also favorable with a mean time of pH <3 of 69 minutes, indicating that dasatinib exposure to highly acidic gastric pH was of sufficient duration to allow drug dissolution yet still temporary. The time course and magnitude of gastric pH change was similar to what was found in our previous methodology study (16). These characteristics with which BHCl lowers gastric pH make it a promising strategy for patients to co-administer BHCl with dasatinib, as greater than 90% of a 150 mg Sprycel tablet was reported to be dissolved within 10 minutes at pH 3 in a previous dissolution study (24).

The increases in dasatinib C_{max} and AUC within an individual subject during BHCl treatment correlated well with the subject's $AUC_{pH<3}$ during BHCl treatment (**Figure 3.2**). Higher values of $AUC_{pH<3}$ indicate a lower gastric pH over a longer period of time and represent a greater efficacy of BHCl in rabeprazole-induced hypochlorhydria (16). Therefore, confirming sufficient gastric acid exposure in subjects may be useful in predicting improvement in dasatinib absorption during rabeprazole-induced hypochlorhydria. However, it is worth noting that large

inter-individual variability (coefficient of variation > 40%) was observed in the pharmacokinetics of dasatinib across all treatments. The variability in dasatinib pharmacokinetics was also observed in the geometric mean ratios, reported in **Table 3.3**. Although the ratios for the treatment comparisons were expected due to the significant differences in gastric pH at the time of dasatinib dosing, the 90% confidence intervals for dasatinib C_{max} and AUCs in the C-to-A comparison fall well outside of the FDA recommended 80-125% confidence interval of no effect. Previous reports have described that the large inter-individual variability may be mostly attributed to drug absorption, more specifically oral bioavailability, that can range from 32% to 118% (25).

The severity of a drug-drug interaction due to changes in gastric pH can be highly drug dependent and governed by a drug's physicochemical properties and the pH range over which its solubility is sensitive. As demonstrated in this study, dasatinib absorption is highly sensitive to gastric pH changes that occur during ARA therapy (pH 4 to 6) since its solubility is dramatically reduced from 18.4 mg/mL at pH 2.6 to 0.008 mg/mL at pH 6.0 (9). Therefore, dasatinib may serve as an example of what could be considered a worst-case scenario and not all small molecule, targeted anti-cancer agents may experience this degree of an interaction, if at all. For example, vandetanib (Calpresa®) is a tyrosine kinase inhibitor used to treat advanced medullary thyroid cancer (26), and although vandetanib also exhibits a pH-dependent solubility (increased solubility at low pH), its highest dose strength of 300 mg is highly soluble in aqueous media until pH 6 at 37°C (27), suggesting that a clinically significant drug-drug interaction between vandetanib and ARAs is not likely. Therefore, we hypothesize that weakly basic drugs with a dynamic pH-dependent solubility between pH 1–4 will be most affected by elevations in gastric pH during concomitant ARA therapy.

Though we demonstrate the success of BHCl to enhance dasatinib absorption under rabeprazole-induced hypochlorhydria, further studies are warranted to investigate the impact that BHCl co-administration will have on dasatinib efficacy in patients with CML also taking ARAs to manage GERD symptoms. It was recently reported that dasatinib major cytogenetic response, defined as having ≤35% of cells test positive for the Philadelphia chromosome (28), was significantly associated with dasatinib steady-state concentrations and maintenance of uninterrupted dosing (29). Thus, a clinical study comparing dasatinib major cytogenetic responses in CML patients taking ARAs with and without gastric acid modulation would be needed to describe the clinical significance of BHCl co-administration to improve drug absorption.

CONCLUSION

Drug-drug interactions between gastric pH and weakly basic drugs with pH-dependent solubility can significantly impact systemic concentrations and drug exposures. However, we report for the first time herein that the use of BHCl, a gastric acid supplement in a solid oral dosage form, can vastly improve dasatinib absorption in healthy volunteers with rabeprazole-induced hypochlorhydria. While the magnitude of the effect may be drug dependent, the results of this study suggest that co-administration of BHCl can be a viable strategy to enhance the absorption of other small molecule, targeted anti-cancer agents that have pH-dependent solubility in the range of pH 1-4 and are given during ARA therapy.

ACKNOWLEDGEMENTS:

The authors would like to acknowledge the staff and nurses of the UCSF-CCRC for their assistance in this study. The UCSF-CCRC is supported by an NIH/NCRR grant (UL1 RR0224131). This study was supported by a grant from Genentech, Inc., and M. R. Yago was supported in part by NIH Training Grant T32 GM007175.

REFERENCES

1. Dressman JB, Vertzoni M, Goumas K, Reppas C. Estimating drug solubility in the gastrointestinal tract. Adv Drug Deliv Rev. 2007;59:591-602.
2. Gawron AJ, Pandolfino JE, Miskevics S, Lavela SL. Proton pump inhibitor prescriptions and subsequent use in US veterans diagnosed with gastroesophageal reflux disease. J Gen Intern Med. 2013;28:930-7.
3. National Center for Health Statistics. Health, United States, 2012: With Special Feature on Emergency Care. 2013.
4. Chin TW, Loeb M, Fong IW. Effects of an acidic beverage (Coca-Cola) on absorption of ketoconazole. Antimicrob Agents Chemother. 1995;39:1671-5.
5. Eley T, Luo FR, Agrawal S, Sanil A, Manning J, Li T, et al. Phase I study of the effect of gastric acid pH modulators on the bioavailability of oral dasatinib in healthy subjects. J Clin Pharmacol. 2009;49:700-9.
6. Zhu L, Persson A, Mahnke L, Eley T, Li T, Xu X, et al. Effect of low-dose omeprazole (20 mg daily) on the pharmacokinetics of multiple-dose atazanavir with ritonavir in healthy subjects. J Clin Pharmacol. 2011;51:368-77.
7. Budha NR, Frymoyer A, Smelick GS, Jin JY, Yago MR, Dresser MJ, et al. Drug absorption interactions between oral targeted anticancer agents and PPIs: is pH-dependent solubility the Achilles heel of targeted therapy? Clin Pharmacol Ther. 2012;92:203-13.
8. Smelick GS, Heffron TP, Chu L, Dean B, West DA, Duvall SL, et al. Prevalence of acid-reducing agents (ARA) in cancer populations and ARA drug-drug interaction potential for molecular targeted agents in clinical development. Mol Pharm. 2013;10:4055-62.

9. US Food and Drug Administration. Dasatinib (Sprycel) Summary Basis of Approval. 2006.
10. US Food and Drug Administration. Erlotinib (Tarceva) Prescribing Information. 2010.
11. US Food and Drug Administration. Gefitinib (Iressa) Prescribing Information. 2004.
12. US Food and Drug Administration. Nilotinib (Tasigna) Prescribing Information. 2013.
13. US Food and Drug Administration. Crizotinib (Xalkori) Prescribing Information. 2013.
14. Jaruratanasirikul S, Kleepkaew A. Influence of an acidic beverage (Coca-Cola) on the absorption of itraconazole. Eur J Clin Pharmacol. 1997;52:235-7.
15. Ray JE, Marriott D, Bloch MT, McLachlan AJ. Therapeutic drug monitoring of atazanavir: surveillance of pharmacotherapy in the clinic. Br J Clin Pharmacol. 2005;60:291-9.
16. Yago MR, Frymoyer AR, Smelick GS, Frassetto LA, Budha NR, Dresser MJ, et al. Gastric reacidification with betaine HCl in healthy volunteers with rabeprazole-induced hypochlorhydria. Mol Pharm. 2013;10:4032-7.
17. Michalek W, Semler JR, Kuo B. Impact of acid suppression on upper gastrointestinal pH and motility. Dig Dis Sci. 2011;56:1735-42.
18. Wedemeyer RS, Blume H. Pharmacokinetic drug interaction profiles of proton pump inhibitors: an update. Drug Saf. 2014;37:201-11.
19. Meyer UA. Metabolic interactions of the proton-pump inhibitors lansoprazole, omeprazole and pantoprazole with other drugs. Eur J Gastroenterol Hepatol. 1996;8 Suppl 1:S21-5.

20. Miura M, Satoh S, Tada H, Habuchi T, Suzuki T. Stereoselective metabolism of rabeprazole-thioether to rabeprazole by human liver microsomes. Eur J Clin Pharmacol. 2006;62:113-7.

21. Brave M, Goodman V, Kaminskas E, Farrell A, Timmer W, Pope S, et al. Sprycel for chronic myeloid leukemia and Philadelphia chromosome-positive acute lymphoblastic leukemia resistant to or intolerant of imatinib mesylate. Clin Cancer Res. 2008;14:352-9.

22. Bristol-Myers Squibb. The Effect of Omeprazole on the Pharmacokinetics of Dasatinib (BMS-354825) in Healthy Subjects. In: ClinicalTrials.gov [Internet]. Bethesda (MD): National Library of Medicine (US). 2000-2014. Available from: http://clinicaltrials.gov/show/NCT00655746: NCT00655746. 2009.

23. Stedman CA, Barclay ML. Review article: comparison of the pharmacokinetics, acid suppression and efficacy of proton pump inhibitors. Aliment Pharmacol Ther. 2000;14:963-78.

24. Fish MP, Young J, Shah P, Gao Z. The use of experimental design principles in dissolution method development: development of a discriminating dissolution method for Sprycel film-coated tablets. J Pharm Innov. 2009;4:165-73.

25. van Erp NP, Gelderblom H, Guchelaar HJ. Clinical pharmacokinetics of tyrosine kinase inhibitors. Cancer Treat Rev. 2009;35:692-706.

26. Grande E, Kreissl MC, Filetti S, Newbold K, Reinisch W, Robert C, et al. Vandetanib in advanced medullary thyroid cancer: review of adverse event management strategies. Adv Ther. 2013;30:945-66.

27. US Food and Drug Administration. Vandetanib (Caprelsa) Summary Basis of Approval. 2011.

28. Kantarjian HM, Smith TL, O'Brien S, Beran M, Pierce S, Talpaz M. Prolonged survival in chronic myelogenous leukemia after cytogenetic response to interferon-alpha therapy. The Leukemia Service. Ann Intern Med. 1995;122:254-61.

29. Wang X, Roy A, Hochhaus A, Kantarjian HM, Chen TT, Shah NP. Differential effects of dosing regimen on the safety and efficacy of dasatinib: retrospective exposure-response analysis of a Phase III study. Clin Pharmacol. 2013;5:85-97.

CHAPTER 4. THE USE OF BDDCS TO EVALUATE THE ROLE OF HEPATIC UPTAKE TRANSPORTERS ON THE DISPOSITION OF TYROSINE KINASE INHIBITORS

ABSTRACT

The Biopharmaceutics Drug Disposition Classification System (BDDCS) separates drugs into one of four classes based on their solubility, extent of metabolism and membrane permeability rate, and can be used to predict potential transporter effects on drug disposition. For small-molecule tyrosine kinase inhibitors (TKIs), previously published transporter studies have focused specifically on their affinities for efflux transporters or their ability to inhibit either uptake or efflux transporters. However, as many TKIs are metabolized in the liver, uncovering the mechanisms of hepatic uptake will provide a greater understanding of the potential factors that may influence hepatic clearance mechanisms and TKI exposure. The goals of this work were: 1) to use *in vitro* permeability studies to define BDDCS class of dasatinib, bosutinib, and vandetanib and 2) to determine the roles of basolaterally expressed hepatic uptake transporters on TKI accumulation using transfected cellular systems and cryopreserved human hepatocytes. Passive permeability rates in Parallel Artificial Membrane Permeability Assays for dasatinib, bosutinib, and vandetanib were 6.82 ± 0.20, 24.9 ± 1.6, and 35.3 ± 3.5 (mean ± SD $x10^{-6}$ cm/s; 25 µM, pH 7.4), respectively, and were found to be higher than labetalol, a BDDCS Class I drug with a known high permeability rate (4.34 ± 0.13 $x10^{-6}$ cm/s; 25 µM, pH 7.4). The TKIs were thus classified as BDDCS Class II drugs due to their high permeability rates and low solubility, and therefore may be affected by uptake or efflux transporter effects in the liver. However, *in vitro* transporter studies of OCT1, OATP1B1, OATP1B3, and OATP2B1 in transfected cellular systems and cryopreserved human hepatocytes revealed neither saturable uptake nor any effects

of known transporter inhibitors on TKI uptake at clinically achievable concentrations. Therefore, we concluded that hepatic uptake of the selected TKIs is mediated only by passive diffusion and uptake transporter-mediated drug-drug interactions will have no impact on the hepatic elimination of dasatinib, bosutinib, and vandetanib.

INTRODUCTION

Over the past decade, an increasing amount of evidence has been published by the scientific community regarding the roles of drug transporters in the *in vivo* disposition of drugs and the clinical impacts they may have (1-3). Drug transporters, which includes both efflux and uptake transporters, are expressed throughout different tissues and major organs of the body including the intestine, liver, kidney, and brain, and have the potential to influence both systemic and intracellular drug concentrations (4-7). Efflux transporters, such as P-glycoprotein (P-gp) and Breast Cancer Resistant Protein (BCRP), reduce intracellular concentrations of xenobiotics by "pumping" them out of the cell irrespective of the existing concentration gradients, but at the cost of ATP (8). In contrast, uptake transporters, such as the members of the Solute Carrier Organic anion (SLCO) transporter family, can transport xenobiotics down an electrochemical gradient from the extracellular to the intracellular space (9).

Drug transporters have also been shown on numerous occasions to have combinatory effects with drug metabolizing enzymes, often referred to as enzyme-transporter interplay (10-12), and can vary based on the transporter in question and its relative position to the enzymes. In the intestine for example, efflux of a drug by P-gp, which is expressed at the apical membranes of enterocytes, provides CYP3A4 more opportunities to metabolize a drug, as the drug must re-permeate enterocytes as it progresses through the small intestine in order to be absorbed (assuming the drug is a substrate of both P-gp and CYP3A4). Thus, inhibition of P-gp would lead to an increased intestinal bioavailability, as CYP3A4 would only have one opportunity to metabolize the drug upon its entry into the enterocyte. The opposite effects would be seen in the liver however, where P-gp is localized at the hepatic apical membranes at the bile canaliculi. In the same situation, a drug molecule that enters hepatocytes would encounter CYP3A4 before P-

gp, and an inhibition of P-gp would cause an accumulation of drug in the hepatocyte, resulting in an increase in drug metabolism and lowered hepatic bioavailability (13).

Therefore it is of great importance in the drug developmental sciences to be able to predict potential transporter effects on drug disposition in the major organ systems, including the intestine and liver. Originally developed by Wu and Benet in 2005, the Biopharmaceutics Drug Disposition Classification System (BDDCS) classifies drugs into four categories, based on their solubility and extent of metabolism, the latter of which is also correlated with intestinal permeability rate (14). The utility of this system lies within its ability to predict potentially clinically relevant transporter effects on drug disposition in tissues, such as the intestine, liver, and brain, based on a drug's respective class. To summarize, Class I drugs are expected to have no clinically significant transporter effects, Class II drugs may be affected by either efflux transporter effects in the intestine or uptake and/or efflux transporter effects in the liver, and Class III and IV drugs may be affected by both uptake and efflux transporter effects (15).

For marketed drugs, BDDCS can thus predict whether transporter-based drug-drug interactions will be clinically significant. Tyrosine kinase inhibitors (TKIs) for example, are a class of compounds typically used as anti-cancer agents for a variety of different cancers (16) and are metabolized by phase I or phase II processes in the liver (17). In addition, TKIs generally have a large inter-individual variability in their pharmacokinetics, much of which can be attributed to variations in oral bioavailability and concomitant administration of drugs that cause interactions with drug metabolizing enzymes and/or transporters (18). Furthermore, rates of polypharmacy for patients prescribed small molecule TKIs have been shown to rise with the occurrence of other health conditions secondary to the cancer, thereby increasing the risks of potential drug-drug interactions that may impact the therapeutic efficacy of the TKI (19).

Though many of the metabolic interactions involving TKIs are known, studies of TKI interactions with drug transporters have mainly focused on their affinity for efflux transporters or their ability to inhibit uptake or efflux transporters (17), and current data are lacking regarding the mechanisms of hepatic uptake of TKIs. Thus the objectives of this work were to use *in vitro* permeability measures to experimentally assign BDDCS classification of dasatinib, bosutinib, and vandetanib (**Figure 4.1**), and to utilize BDDCS to determine the roles of hepatic uptake transporters in TKI drug disposition.

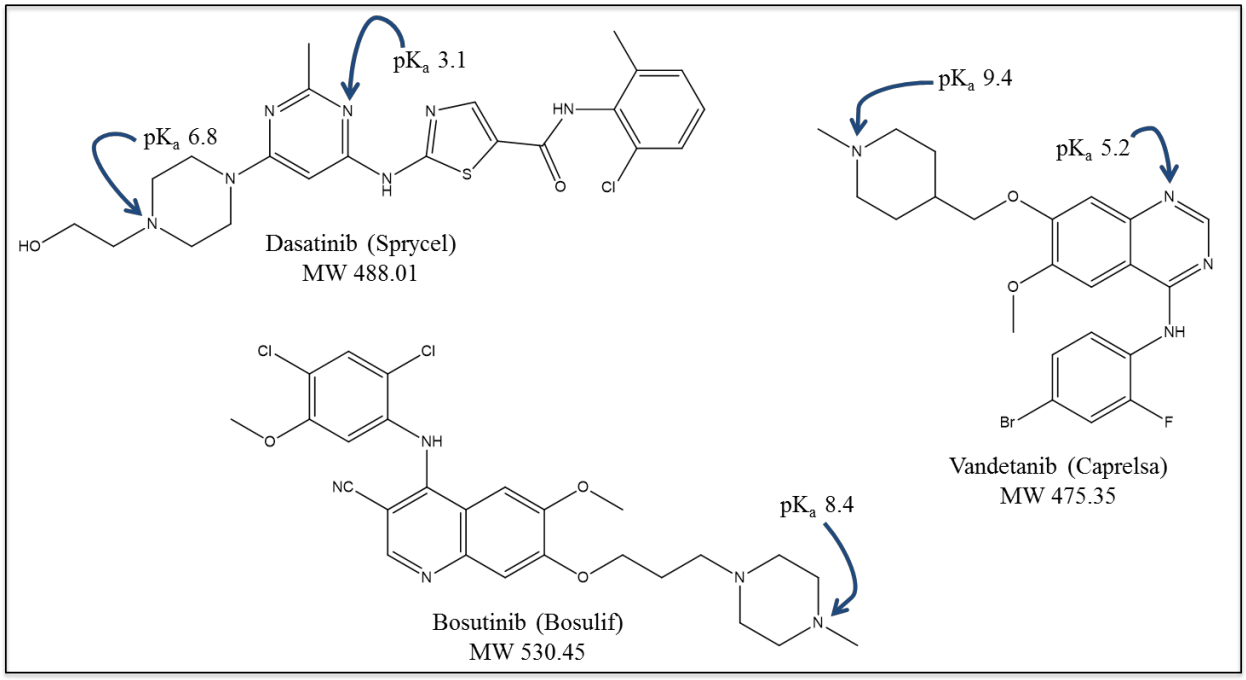

Figure 4.1 Structures of dasatinib, bosutinib, and vandetanib.

EXPERIMENTAL

Chemicals

[^{3}H]-Estrone-3-sulfate (Estrone Sulfate, Ammonium Salt-,[6,7-^{3}H(N)]-, 250 µCi (9.25 MBq), NET203250UC; Lot 1609304) and [^{3}H]-estradiol-17β-glucuronide (Estradiol 17 β-D-

Glucuronide,[Estradiol-6,7-^{3}H(N)]-, 50 µCi (1.85 MBq) NET1106050UC; Lot 1645534) were purchased from Perkin Elmer Inc. (Boston, MA). Carbamazepine (C4024-5G), cimetidine (C4522), labetalol (labetalol hydrochloride, L1011), metformin (1,1-dimethylbiguanide hydrochloride, D5035), rifampicin (R3501-G), rifamycin-SV (sodium salt, 83909), and verapamil (±-verapamil hydrochloride, V-4629) were purchased from Sigma-Aldrich (St. Louis, MO). GG918 (elacridar, SRP01030e) was purchased from Sequoia Research Products (Pangbourne, United Kingdom). Dasatinib (D193600), bosutinib (B676095), vandetanib (V097100), and the internal standard pazopanib (P210925) were purchased from Toronto Research Chemicals (Toronto, Ontario, Canada).

Cell Culture Conditions

Caco-2 cells (American Type Culture Collection, Rockville, MD) were cultured as previous described (20). To summarize, Caco-2 cells were grown in Minimal Essential Eagle's Medium (MEM) containing L-glutamine (2 mM), glucose (5.5 mM), sodium bicarbonate (2.6 mM), sodium pyruvate (1.0 mM), nonessential amino acids (0.1 mM), penicillin and streptomycin (100 U/mL), and 10% heat-inactivated fetal bovine serum. Caco-2 cells were seeded onto BD Falcon^{TM} polyethylene terephthalate inserts (0.4 µm pore size for 6-well plates; BD Biosciences, San Jose, CA) at a density of 250,000 cells per insert and grown to confluence for 21-23 days. Cell media were changed 24 hours after seeding, thrice weekly, and 24 hours prior to experiments.

HEK-293 cells were stably transfected with *SLCO1B1* (OATP1B1), *SLCO1B3* (OATP1B3), or *SLCO2B1* (OATP2B1) using the pCI-neo mammalian vector (Promega, Madison, WI) and cultured in Dulbecco's Modified Eagle Medium containing 10% heat-

inactivated fetal bovine serum, penicillin/streptomycin (100 U/mL), and Geneticin® (0.5 mg/mL; UCSF Cell Culture Facility, San Francisco, CA). HEK-293 cells stably transfected with *SLC22A1* (OCT1) were generously provided by Dr. Kathleen Giacomini (UCSF, San Francisco, CA) and cultured as previously described (21).

HEK-293 cells expressing OATP1B1, OATP1B3, OATP2B1, or OCT1 were seeded at approximately 0.5 x 10^6 cells/mL in each well of poly-D-lysine coated 12-well plates (BD Biosciences, San Jose, CA). Approximately 48 hours after seeding, cell media were changed to fresh growth media not containing any selection markers. In the case of OATP1B3-expressing cells, the media were changed to growth media containing sodium butyrate (10 mM). Uptake studies were then performed within 24 hours.

Transport buffer for all experiments consisted of Hank's Balanced Salt Solution without phenol red, supplemented with 1% fetal bovine serum (v/v) and either HEPES (25 mM, pH 7.4) or N-morpholino ethanesulfonic acid (20 mM, pH 6.5), pH-adjusted using 1 N sodium hydroxide. Dosing solutions for all compounds were made fresh on the morning of each experiment and contained less than 1% and 0.1% DMSO for PAMPA and cellular experiments, respectively.

In Vitro Permeability Studies Using the Parallel Artificial Membrane Permeability Assay (PAMPA) and Caco-2 Cell Monolayers

Permeability studies in PAMPA were based on the original protocol described in the BD Biosciences Guidelines for Use (22). All drug dosing solutions were prepared at concentrations of 25 and 50 µM at pH 6.0 and 7.4 in phosphate-buffered saline (PBS). In each well of the donor plate, 0.3 mL of drug dosing solution was added, with 0.2 mL of blank PBS added to each well

of the receiver plate. To initiate the study, the plates were assembled together and placed in an incubator at 37°C for 5 hours. After incubation, the study was terminated by separating the donor and receiver plates. In all studies, the pH was held constant across donor and receiver wells.

At the end of the study, 40 µL aliquots from both donor and receiver wells were transferred to separate 96-well plates and diluted with 160 µL of acetonitrile (ACN) containing 0.1% formic acid. An equivalent of ACN containing 0.1% formic acid and internal standard was then added. Samples were vortexed and centrifuged at 13,000x g for 15 minutes prior to LC-MS/MS analysis.

Caco-2 permeability studies were conducted 21-23 days after seeding as previously described (23). To assess the integrity of the monolayers, transepithelial electrical resistance (TEER) values for each well were measured in triplicate on the day of each experiment using a Millipore Millicell®-ERS Voltohmmeter (Millipore Corporation, Bedford, MA). Inserts whose TEER values averaged less than 300 Ω were discarded.

Cells were preincubated with 2 mL and 3 mL of transport buffer in the apical and basolateral chambers, respectively, at 37°C for 30 minutes. After preincubation, inserts were decanted and transferred to new plates containing 2.5 mL of fresh, prewarmed transport buffer in the basolateral chambers. Unidirectional permeability studies (A→B) were initiated with the addition of 1.5 mL of drug dosing solution with or without 1 µM GG918, at pH 7.4 or pH 6.5 in the apical chamber. Aliquots of 200 µL were taken from the apical chamber immediately after dosing and at the end of the experiment (90 minutes). At 30, 60, and 90 minutes, 200 µL aliquots were taken from basolateral chambers and replaced with fresh, prewarmed transport

buffer. Immediately following the final timepoint, inserts were decanted of drug dosing solutions, washed three times with ice-cold PBS, and allowed to dry overnight.

Samples were prepared for LC-MS/MS analysis by diluting 50 µL of each sample with an equivalent of ACN containing 0.1% formic acid and internal standard. To measure intracellular amounts, dried membranes were cut out from each insert, submerged in 1 mL of a mixture of ACN with 25% water, and sonicated for 15 minutes. Following sonication, a 50 µL sample was taken and an equivalent of ACN containing 0.1% formic acid and internal standard was added. All samples were then vortexed and centrifuged at 13,000x g prior to LC-MS/MS analysis.

Uptake Studies Using Transfected Cellular Models

Cells were first washed with transport buffer and preincubated at 37°C for 10 minutes with shaking. Following this, buffer was aspirated and uptake studies were initiated via the addition of 0.6 mL of drug dosing solution. Plates were incubated for designated times and uptake studies were terminated by the aspiration of dosing solutions. Immediately afterwards, each well was washed thrice with ice cold PBS, followed by the addition of 200 µL of D-PBS. Cells were then scraped and transferred to preweighed Eppendorf tubes and re-weighed.

Each sample was homogenized via sonication prior to sample preparation for LC-MS/MS analysis. A 50 µL aliquot of the homogenate was taken, to which 100 µL of ACN containing 0.1% formic acid and internal standard was added. Samples were vortexed for 1 minute and centrifuged for 15 minutes at 13,000 x g. To further facilitate protein precipitation, samples were then stored at -20°C for 30 minutes, followed by another round of centrifugation, prior to LC-MS/MS analysis.

For radiolabeled compounds ([^{3}H]-Estrone-3-sulfate and [^{3}H]-Estradiol-17β-glucuronide), 200 µL of 1% Triton X-100 (Fisher BioReagents®, Fair Lawn, New Jersey) was added to each well after PBS washings to detach cells from the plates. Contents were then transferred to individual scintillation vials, to which 5 mL of Econo-Safe scintillation cocktail (RPI Corp., Mount Prospect, IL) was added. Radioactivity was then measured with a liquid scintillation counter (LS 6000TA, Beckman Coulter).

Protein measurements were conducted using a Pierce Micro BCA Protein Assay Kit (Thermo Scientific, Waltham, MA).

Inhibition of Hepatic Uptake Transporters in Cryopreserved Human Hepatocytes

Cryopreserved human hepatocytes (Triangle Research Laboratories, Durham, NC) were used in suspension for all uptake studies. Hepatocytes were first flash thawed in a water bath at 37°C for no longer than 2 minutes. Once liquefied, contents were added to 5 mL of prewarmed Williams Media E, supplemented with dexamethasone (0.1 µM) and a cell maintenance cocktail (Life Biotechnologies, Grand Island, NY) that included HEPES (15 mM), glutamine (2 mM), and penicillin/streptomycin (0.5%). Hepatocyte yield and cell number were determined using the Trypan Blue Exclusion method, upon which hepatocytes were then diluted with prewarmed media to 1 x 10^6 cells/mL.

Drug dosing solutions consisted of dasatinib, bosutinib, or vandetanib with and without the inhibitors rifampicin or cimetidine. In each experiment, the final concentrations of all TKIs were 1 µM, while the final concentrations of rifampicin and cimetidine were 20 and 300 µM, respectively. Additionally, inhibition studies were conducted with matched controls using hepatocytes from the same lot.

In a 24-well plate, 0.5 x 10^6 cells were added to individual wells and preincubated at 37°C (with shaking) for 10 minutes. After preincubation, 0.5 mL of drug dosing solution with or without inhibitor was added to initiate the uptake study and plates were placed back into the incubator. At the end of the incubation, a 0.5 mL aliquot was taken and added to Eppendorf tubes containing a mixture of silicone and mineral oil (density = 1.05 g/mL). Samples were centrifuged at 13,000 x g for 30 seconds to pellet hepatocytes, and the oil/media supernatant was promptly removed.

Hepatocyte pellets were resuspended in 300 µL of water and sonicated for 15 minutes to lyse cells. Samples were then prepared for LC-MS/MS analysis as described for HEK-293 experiments.

Measurement of Drug Concentrations via LC-MS/MS

Dasatinib, bosutinib, vandetanib, labetalol, and metformin were all measured using LC-MS/MS methods with a Shimadzu LC20-AD HPLC system (Shimadzu, Kyoto, Japan) coupled to an API 4000 triple quadrupole mass spectrometer (Applied Biosystem/MDS Sciex, Framingham, MA) using electrospray ionization operating in the positive ion mode.

Detection of TKIs was performed on a reverse phase column (Zorbax XDB-C18, 5 µm, 4.6 x 50 mm; Agilent, Santa Clara, CA) using a gradient of water and ACN each containing 0.1% formic acid, over 7.5 minutes with a flow rate of 0.5 mL/min. Quantification was performed using multiple reaction monitoring (MRM) with the following mass transitions: MH^+ m/z 488→401 for dasatinib, MH^+ m/z 531→141 for bosutinib, MH^+ m/z 475→112 for vandetanib, and MH^+ m/z 438→357 for pazopanib (internal standard).

Detection of labetalol and metformin were both performed on a reverse phase column (Zorbax XDB-C8, 3.5 µm, 4.6 x 50 mm; Agilent, Santa Clara, CA) with a gradient of water and ACN, each containing 0.1% formic acid. At a flow rate of 0.5 mL/min, the gradient lasted 6 minutes for labetalol and 5 minutes for metformin. Quantification was also performed using MRM with the following mass transitions: MH^+ m/z 329→162 for labetalol and MH^+ m/z 130→71.0 for metformin. Carbamazepine was used as an internal standard for both methods, with mass transition MH^+ m/z 237→194.

Data Analyses

Permeability rates (P_{app}) for PAMPA experiments were calculated using the following equation, as directed in the BD Biosciences Guidelines for Use (22):

$$P_{app} = \frac{-\ln\left[1 - \frac{C_R(t)}{C_{eq}}\right]}{A * \left(\frac{1}{V_D} + \frac{1}{V_R}\right) * t}$$

where $C_{eq} = \frac{[C_D(t) * V_D] + [C_R(t) * V_R]}{V_D + V_R}$, $C_R(t)$ and $C_D(t)$ are the concentrations in the receiver and donor wells at time t, respectively, and V_R and V_D are the volumes in the receiver and donor wells, respectively. In Caco-2 experiments, P_{app} values were calculated as previously described (23):

$$P_{app} = \frac{dM}{dt} * \frac{1}{C_0} * \frac{1}{A}$$

where $\frac{dM}{dt}$ is the amount of drug that appears in the receiving well over time, C_0 is the initial concentration in the donor well, and A is the area of the filter. All P_{app} values are reported in units of cm/s. Statistically significant differences in P_{app} values were determined using a one-way analysis of variance with $\alpha = 0.05$ and Dunnett's correction for multiple comparisons.

Uptake rates (V_0) for studies conducted in transfected HEK-293 cells were calculated as follows:

$$V_0 = \frac{C * V_{sample}}{t * M_{prot.}}$$

where C is the measured intracellular drug concentration, V_{sample} is the volume of the cell suspension (assuming a density of 1 mg/mL), t is the length of the uptake study, and $M_{prot.}$ is the measured protein amount. Concentration versus V_0 curves were then analyzed using non-linear regression analyses in Prism 5 for Windows (GraphPad, La Jolla, CA) to determine Michaelis-Menten parameters (K_M and V_{max}). Statistically significant differences in V_0 between control and inhibitor groups were determined using a two-tailed *t*-test with $\alpha = 0.05$ in Prism 5 for Windows (GraphPad, La Jolla, CA).

Uptake rates for studies in cryopreserved human hepatocytes were calculated in a similar fashion and were reported as the percent of control (no inhibition). A one-way analysis of variance with $\alpha = 0.05$ and Dunnett's correction for multiple comparisons (Prism 5 for Windows; GraphPad, La Jolla, CA) were used to detect statistically significant differences in uptake rates between control and inhibited groups.

RESULTS

Permeability Studies in PAMPA and Caco-2

As shown in **Table 4.1**, all 3 TKIs were shown to have higher P_{app} values than the high permeability rate compound, labetalol, at each concentration and pH tested in PAMPA. Furthermore, there were significant pH effects between experiments conducted at pH 6.0 and pH 7.4, with all compounds exhibiting higher P_{app} values at pH 7.4 compared to pH 6.0 ($P < 0.05$).

In Caco-2 permeability studies however, the opposite trends were observed, with TKIs exhibiting significantly lower $P_{app, A\rightarrow B}$ values relative to labetalol (**Table 4.2**). Interestingly, the pH effect in TKI P_{app} that was formerly present in PAMPA experiments no longer existed in Caco-2 studies at both of the dosing concentrations used. However, labetalol did exhibit significantly higher $P_{app, A\rightarrow B}$ values when dosed at pH 7.4 compared to pH 6.5 for the 2 µM dose and 4 µM dose treated with GG918 (P <0.001). Data for 2 µM bosutinib studies were not determined due to measured concentrations below the lower limit of quantification.

Table 4.1 Apparent permeability rates (P_{app}) measured in PAMPA at pH 6.0 and pH 7.4.

Drug	25 µM Dose			50 µM Dose		
	pH 6.0	**pH 7.4**	**pH Effect?**	**pH 6.0**	**pH 7.4**	**pH Effect?**
Dasatinib	1.57 ± 0.09 **	6.82 ± 0.20 N.S.	††	1.32 ± 0.22 N.S.	6.13 ± 0.79 N.S.	†††
Bosutinib	6.58 ± 0.59 ***	24.9 ± 1.6 ***	†††	4.20 ± 0.25 ***	14.1 ± 1.0 ***	†††
Vandetanib	8.01 ± 0.27 ***	35.3 ± 3.5 ***	†††	7.57 ± 1.07 ***	22.1 ± 1.1 ***	†††
Labetalol	0.417 ± 0.012	4.34 ± 0.13	†	0.615 ± 0.063	4.43 ± 0.38	†††

P_{app} values are expressed as the means ± SD of two replicates performed in triplicate, in units of $x10^{-6}$ cm/s. Labetalol, a BDDCS Class I drug, was used as a positive control and a reference standard for compounds with a high permeability rate. In each experiment, the pH was held constant across donor and receiver wells. Asterisks (*) indicate statistically significant differences in P_{app} when compared to labetalol, while daggers (†) indicate statistically significant differences in P_{app} between pH 6.0 and pH 7.4 when dosed at the same concentration. N.S., Not significant; †P <0.05; **/††P <0.01; ***/†††P <0.001

To assess the potential involvement of efflux transporter effects (namely P-gp and BCRP), GG918 was co-administered with a final concentration of 1 µM (**Figure 4.2**). As shown, GG918 did not have any effect on $P_{app, A\rightarrow B}$ values for any of the TKIs tested at both pH 6.5 and pH 7.4, despite significantly increasing labetalol $P_{app, A\rightarrow B}$ at pH 7.4 (P <0.05).

Of note, in both PAMPA and Caco-2 experiments, dasatinib consistently exhibited the lowest P_{app} values for all dosing conditions amongst the TKIs, followed by bosutinib and vandetanib.

Uptake Studies in HEK-293 Cells Overexpressing OATPs

As shown in **Figure 4.3**, dasatinib, bosutinib, and vandetanib did not show any saturable uptake in HEK-293 cells overexpressing human OATPs in the concentration range 0.02–50 µM. Furthermore, when dosed concomitantly with the OATP inhibitor rifamycin-SV, no significant differences in V_0 were observed for the majority of substrate concentrations tested, despite the greater than 50% reductions observed in the uptake of [^{3}H] estrone-3-sulfate and [^{3}H] estradiol-17β-glucuronide. Because of the linearity observed in V_0 with increasing substrate concentrations, K_M and V_{max} could not be estimated.

Interestingly, the rate of dasatinib uptake for all OATPs investigated were consistently lower than bosutinib and vandetanib, similar to trends observed in PAMPA and Caco-2 permeability studies.

Table 4.2 Unidirectional (A→B) apparent permeability rates ($P_{app, A→B}$) measured in Caco-2 cell monolayers at pH 6.5 and pH 7.4

Drug	2 µM Dose		4 µM Dose		4 µM Dose + GG918 (1 µM)	
	pH 6.5	pH 7.4	pH 6.5	pH 7.4	pH 6.5	pH 7.4
Dasatinib	0.666 ± 0.033	0.702 ± 0.042	0.771 ± 0.043	0.708 ± 0.034	0.769 ± 0.077	0.780 ± 0.010
Bosutinib	ND	ND	0.162 ± 0.009	0.172 ± 0.011	0.161 ± 0.045	0.216 ± 0.045
Vandetanib	0.241 ± 0.006	0.258 ± 0.012	0.223 ± 0.018	0.267 ± 0.013	0.232 ± 0.014	0.232 ± 0.089
Labetalol	1.23 ± 0.02	1.78 ± 0.06 ***	1.61 ± 0.46	2.28 ± 0.17	1.62 ± 0.04	2.78 ± 0.08 ***,†

$P_{app, A→B}$ values are expressed as the means ± SD of two replicates performed in triplicate, in units of $x10^{-6}$ cm/s. The pH values of each column indicate the pH at which each drug was dosed in the apical chambers, while the pH of all basolateral (receiver) chambers was held constant at pH 7.4. Similar to PAMPA, labetalol was used as a positive control and reference standard for drugs with high permeability rates. Each experiment was conducted over a time course of 90 minutes. No significant differences in $P_{app,A→B}$ were observed between dosing (apical) pH or efflux transporter inhibition via GG918 for the TKIs. However, significant differences in labetalol $P_{app,A→B}$ were observed between dosing (apical) pH at the 2 µM dose and 4 µM dose treated with GG918 (***P <0.001). In addition, efflux transporter inhibition via GG918 significantly increased labetalol $P_{app,A→B}$ when dosed at pH 7.4 (†P <0.05).
ND, Not determined (below lower limit of quantification)

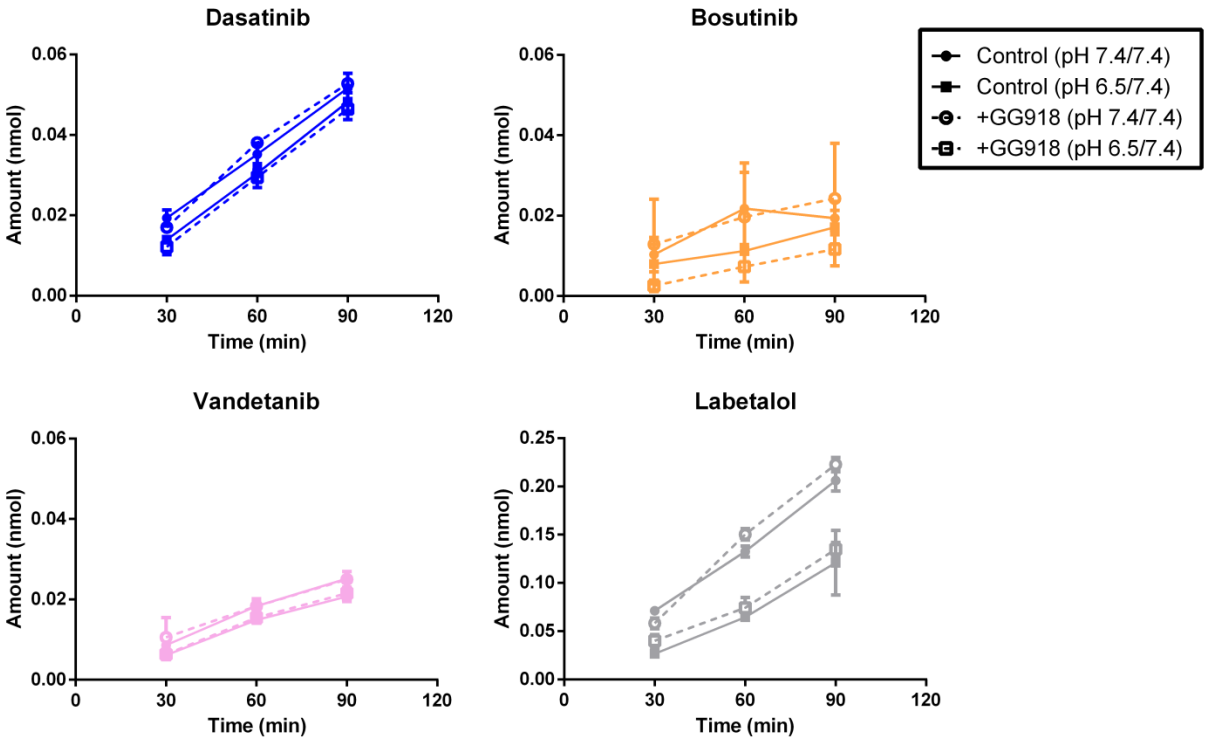

Figure 4.2 Rate of appearance of drug in unidirectional (A→B) permeability studies conducted in Caco-2 cell monolayers. Dasatinib, bosutinib, vandetanib, and labetalol were dosed in apical wells at either pH 6.5 (-■-) or pH 7.4 (-●-), in the absence (filled shapes) or presence (empty shapes) of the efflux transporter inhibitor GG918 (final concentration, 1 µM). Data are plotted as the means ± SD of two replicates performed in triplicate and lines are only for graphical purposes.

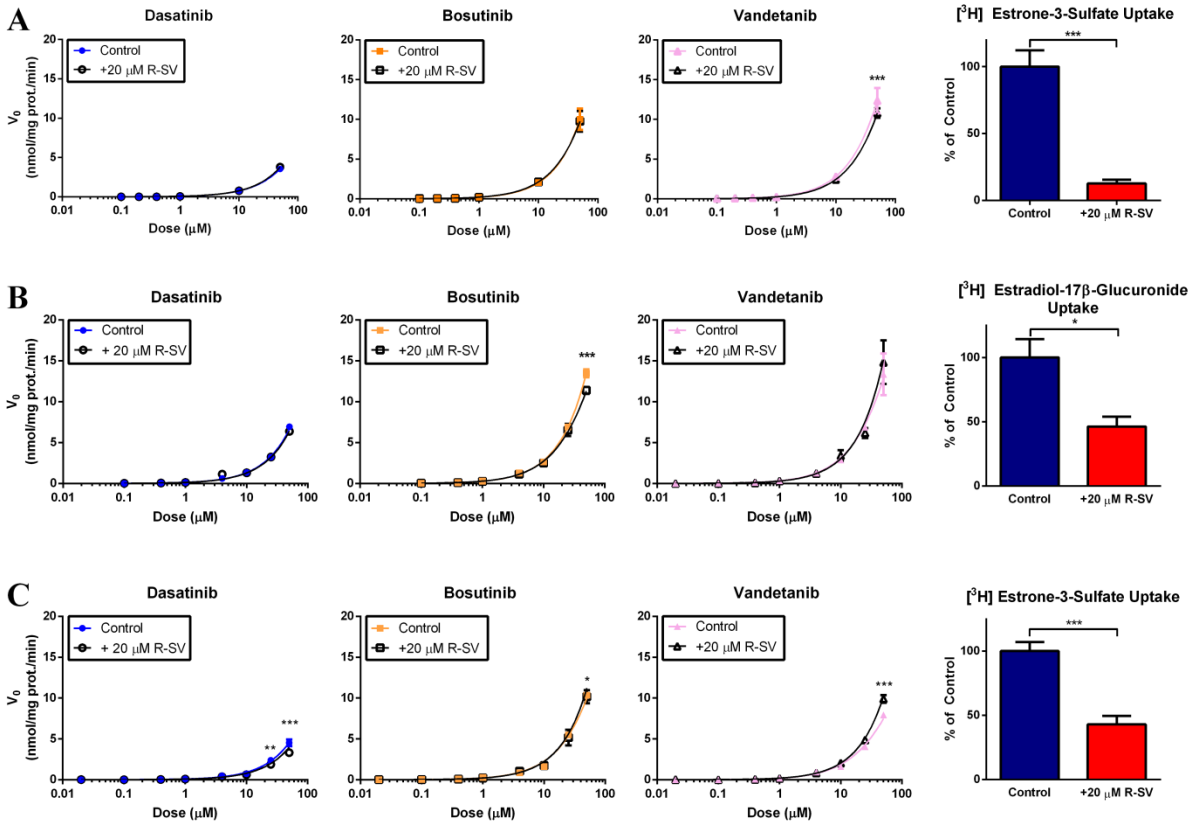

Figure 4.3 Measured uptake rates of dasatinib, bosutinib, and vandetanib in HEK-293 cells overexpressing (A) OATP1B1, (B) OATP1B3, and (C) OATP2B1. Uptake studies in each of the transfected cell lines were conducted within the linear range of uptake (1 min) using substrate concentrations of 0.02–50 µM, in the absence (closed, colored shapes) and presence (open, black shapes) of the OATP inhibitor rifamycin-SV (20 µM). Uptake of [^{3}H] estrone-3-sulfate was used as positive control for OATP1B1 and OATP2B1 cell lines, whereas [^{3}H]-estradiol-17β-glucuronide uptake was used for OATP1B3 cell lines. Statistically significant differences between control and inhibited groups are indicated with asterisks: **P* <0.05; ***P* <0.01; ****P* <0.001. Data are represented as the means ± SD.

Uptake Studies in HEK-293 Cells Overexpressing OCT1

Figure 4.4 depicts the uptake rates of dasatinib, bosutinib, and vandetanib in HEK-293 overexpressing OCT1. Similar to the studies in OATP cell lines, the TKIs did not exhibit saturable uptake in the concentration range of 0.02–50 µM, and as such, K_M and V_{max} could not be estimated. Additionally, the OCT1 inhibitor verapamil had no effect on the accumulation of the TKIs, despite significantly reducing metformin uptake to less than 25% of the control (*P* <0.001).

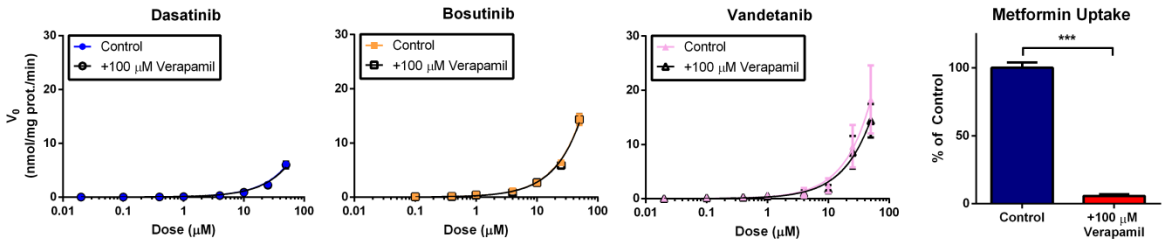

Figure 4.4 Uptake rates of dasatinib, bosutinib and vandetanib in HEK-293 cells overexpressing OCT1. Uptake studies were conducted in the linear range of uptake (1 min) using substrate concentrations ranging from 0.02–50µM, in the absence (closed, colored shapes) and presence (open, black shapes) of the OCT1 inhibitor, verapamil (100 µM). Metformin uptake was used as a positive control to assess transporter function, and data are expressed as the means ± SD.

Inhibition of Uptake Transporters in Cryopreserved Human Hepatocytes

Figure 4.5 summarizes the effects of OATP (OATP1B1, OATP1B3, and OATP2B1) and OCT1 inhibition in cryopreserved human hepatocytes using 20 µM rifampicin and 300 µM

cimetidine, respectively. Although cell viability after thawing averaged greater than 80% on each occasion, no significant differences in uptake rates were observed.

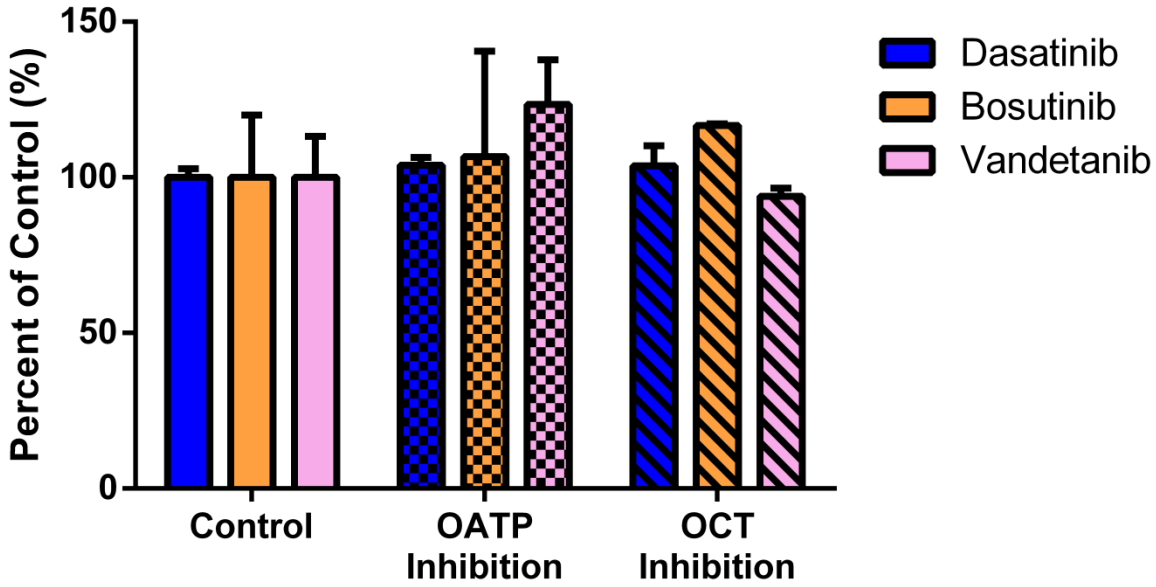

Figure 4.5 Effect of OATP and OCT1 inhibition on the uptake rates of dasatinib, bosutinib, and vandetanib in cryopreserved human hepatocytes. Cryopreserved human hepatocytes were used to assess the effects of inhibition of OATPs (checkered bars) and OCT1 (slashed bars) on the accumulation of dasatinib, bosutinib, and vandetanib (final concentration, 1 µM). OATPs were inhibited using 20 µM rifampicin, whereas OCT1 was inhibited using 300 µM cimetidine (final concentrations). Uptake studies were conducted within the linear range of uptake (1 min) and data are expressed as percentages normalized to control (mean ± SD).

DISCUSSION

In this work, dasatinib, bosutinib, and vandetanib exhibited high passive permeability rates in comparison to labetalol, and with their low solubilities, were classified as BDDCS Class II drugs. Although the drug disposition of BDDCS Class II drugs may be affected by transporter effects in the intestine and liver, hepatic uptake transporter studies with human OATP1B1, OATP1B3, OATP2B1, and OCT1 revealed neither saturable uptake nor effects of transporter inhibition, suggesting that passive diffusion is the primary route that these selected TKIs use to enter the liver for subsequent metabolism.

The solubility criterion of BDDCS and the previously established Biopharmaceutics Classification System (BCS) follows the FDA Guidance for Industry and deems a drug as "highly soluble" when its highest dose strength is soluble in 250 mL or less of aqueous media over the pH range 1–7.5 at 37°C (24). Dasatinib, bosutinib, and vandetanib were previously identified as poorly soluble drugs in BCS (25-27) and thus are designated as poorly soluble in BDDCS as well. The TKIs also show significantly higher P_{app} values in PAMPA relative to the BDDCS Class I drug labetalol, with all drugs exhibiting a higher permeability rate at pH 7.4 versus pH 6.0. As basic drugs, these significant pH effects can be attributed to the larger fraction of nonionized species in solution at pH 7.4 as described by the pH-partition hypothesis. With P_{app} values higher than labetalol, the TKIs were designated as high permeability rate and extensively metabolized drugs, as our laboratory has previously shown that passive permeability rates can predict extent of metabolism (28). Thus in conjunction with their low solubility, dasatinib, bosutinib, and vandetanib were classified as BDDCS Class II drugs.

Although the TKI permeability rates measured in PAMPA were capable of distinguishing between high and low permeability rate drugs, there were obvious discrepancies between the

permeability rates of the TKIs observed in PAMPA and Caco-2 cells. Strikingly, while the TKIs exhibited significant pH effects and higher permeability rates than labetalol in PAMPA, the opposite was observed in Caco-2 monolayers. The reduced permeability rates in Caco-2 monolayers were thought to be due to potential TKI efflux by P-gp or BCRP, but no significant differences in the A→B permeability rates were observed when co-incubated with the efflux transporter inhibitor, GG918 (**Table 4.2**).

We hypothesize therefore that perhaps the trend differences between the two assays might be attributed to the effects of protein binding on passive drug permeability. Aside from the membrane differences between PAMPA and Caco-2 monolayers, the use of protein in each assay also differs. Drug dosing solutions and blank buffers used in PAMPA experiments were made in PBS and were devoid of any soluble proteins (i.e. fetal bovine serum). However, buffers used in Caco-2 experiments included 1% fetal bovine serum, which in addition to any of the proteins expressed in Caco-2 cells, might produce lower permeability rates for drugs with high protein binding. Dasatinib, bosutinib, and vandetanib, along with many of the other TKIs, are reported to be extensively bound to α_1-acid glycoprotein or albumin in plasma, at levels greater than 98% (17, 18, 25-27), which is nearly twice the reported fraction of labetalol plasma protein binding (50%, (29)). Further investigations to elucidate the relationships between permeability rates and protein binding in these systems are thus warranted.

The opposing trends in permeability rates observed in PAMPA and Caco-2 do highlight some of the limitations of using the Caco-2 system to predict intestinal permeability rate *in vitro*. While BDDCS can use passive permeability rate or extent of metabolism to delineate high versus low intestinal permeability rate drugs, BCS uses extent of absorption (30). Although a high

permeability rate correlates well with a high extent of absorption, there are a number of cases where low permeability rate drugs are also highly absorbed (14).

Sotalol is a notable example of this as it has been shown *in vitro* using Caco-2 monolayers to have a low permeability rate, despite being nearly completely absorbed in humans after oral administration (31). The discrepancy in this result was attributed in part to the low lipophilicity of sotalol and increased tightness of tight junctions in Caco-2 monolayers relative to the jejunum of the intestine (32). Thus the use of Caco-2 monolayers to predict the extent of absorption may lead to an incorrect BCS classification for drugs that undergo paracellular or carrier-mediated transport, or drugs that are either hydrophilic or have poor lipophilicity (32).

For BDDCS Class II drugs (poorly soluble, extensively metabolized), inhibition of hepatic uptake transporters can result in a reduced hepatic clearance, and consequently, increased drug exposures, in situations where drug uptake is rate-limiting (13, 33). For example, previous studies from our laboratory have shown that for atorvastatin, a substrate of OATP1B1, inhibition of uptake via rifampin significantly increased atorvastatin exposure by greater than 6-fold in healthy volunteers (34). This interaction is of particular interest for statins as prolonged exposures have been associated with an increased incidence of statin-induced myopathies (35). Similarly for the anti-diabetic drug metformin, previous studies have shown that the expression of reduced function alleles of OCT1 in the liver contribute to elevated systemic concentrations and reduced therapeutic activity of metformin in humans, highlighting the role of OCT1 in metformin pharmacokinetics and pharmacodynamics (36, 37).

Although dasatinib, bosutinib, and vandetanib were classified as Class II drugs, uptake studies with human OCT1 and OATPs (-1B1, -1B3, and -2B1) revealed no evidence of saturable uptake within the concentration ranges used (**Figures 4.3 and 4.4**), indicating that the TKIs rely

primarily on passive diffusion to enter hepatocytes at clinically relevant concentrations. This was further supported by the inability of OCT1 and OATP inhibitors to cause any significant changes in uptake rates in transfected cell lines and cryopreserved human hepatocytes (**Figure 4.5**). Collectively, these results indicate that transporter-mediated drug-drug interactions between these TKIs and basolaterally expressed hepatic uptake transporters are unlikely to result in significant changes in the exposures of dasatinib, bosutinib, or vandetanib. While many of the small-molecule TKIs share similar physicochemical properties, each TKI should be assessed for potential transporter effects on a case-by-case basis to avoid any erroneous generalizations.

However, despite the lack of dependence on uptake transporters for hepatic uptake, TKIs may still be able to initiate drug-drug interactions with other drugs whose disposition is carrier-mediated. Previous *in vitro* studies have shown that many of the TKIs, including dasatinib and bosutinib, are capable of inhibiting uptake transporters of the SLC family, including OATP1B1 and OCT1, at clinically achievable concentrations (21, 38), which could result in reduced clearance mechanisms or pharmacologic activity of substrate drugs at the organs of elimination or site of action, respectively. In addition, many TKIs can inhibit efflux transporters such as P-gp and BCRP, which may result in increased or decreased intracellular concentrations of substrate drugs, depending on the site of the interaction. Therefore, interactions of TKIs as inhibitors of drug transporters is still a major point of concern due to the frequency of concomitant drug administration during TKI therapy and increased likelihood of potentially clinically significant drug-drug interactions.

CONCLUSION

Dasatinib, bosutinib, and vandetanib were classified as BDDCS Class II drugs due to their low solubility and extensive metabolism and as such, may be subject to efflux transporter effects in the intestine or uptake and/or efflux transporter effects in the liver. However, the data presented herein showed no significant contributions of OATP1B1, OATP1B3, OATP2B1, or OCT1 as evidenced by the lack of saturable uptake with increasing concentrations and lack of effect on uptake rates when coadministered with known inhibitors in transfected cell lines and cryopreserved human hepatocytes, as well as no significant contribution of the efflux transporters P-gp and BCRP when an inhibitor of these transporters was tested. Collectively, we conclude that the uptake of dasatinib, bosutinib, and vandetanib into the liver is mediated only by passive diffusion and uptake transporter-mediated drug-drug interactions will have no impact on the hepatic elimination of these TKIs.

REFERENCES

1. Giacomini KM, Huang SM, Tweedie DJ, Benet LZ, Brouwer KL, Chu X, et al. Membrane transporters in drug development. Nat Rev Drug Discov. 2010;9:215-36.
2. Grover A, Benet LZ. Effects of drug transporters on volume of distribution. AAPS J. 2009;11:250-61.
3. Nigam SK. What do drug transporters really do? Nat Rev Drug Discov. 2015;14:29-44.
4. Hilgendorf C, Ahlin G, Seithel A, Artursson P, Ungell AL, Karlsson J. Expression of thirty-six drug transporter genes in human intestine, liver, kidney, and organotypic cell lines. Drug Metab Dispos. 2007;35:1333-40.
5. Morrissey KM, Stocker SL, Wittwer MB, Xu L, Giacomini KM. Renal transporters in drug development. Annu Rev Pharmacol Toxicol. 2013;53:503-29.
6. Geier EG, Chen EC, Webb A, Papp AC, Yee SW, Sadee W, et al. Profiling solute carrier transporters in the human blood-brain barrier. Clin Pharmacol Ther. 2013;94:636-9.
7. Estudante M, Morais JG, Soveral G, Benet LZ. Intestinal drug transporters: an overview. Adv Drug Deliv Rev. 2013;65:1340-56.
8. Glavinas H, Krajcsi P, Cserepes J, Sarkadi B. The role of ABC transporters in drug resistance, metabolism and toxicity. Curr Drug Deliv. 2004;1:27-42.
9. Hediger MA, Romero MF, Peng JB, Rolfs A, Takanaga H, Bruford EA. The ABCs of solute carriers: physiological, pathological and therapeutic implications of human membrane transport proteinsIntroduction. Pflugers Arch. 2004;447:465-8.
10. Cummins CL, Jacobsen W, Benet LZ. Unmasking the dynamic interplay between intestinal P-glycoprotein and CYP3A4. J Pharmacol Exp Ther. 2002;300:1036-45.

11. Benet LZ, Cummins CL, Wu CY. Transporter-enzyme interactions: implications for predicting drug-drug interactions from in vitro data. Curr Drug Metab. 2003;4:393-8.

12. Benet LZ, Cummins CL, Wu CY. Unmasking the dynamic interplay between efflux transporters and metabolic enzymes. Int J Pharm. 2004;277:3-9.

13. Benet LZ. The drug transporter-metabolism alliance: uncovering and defining the interplay. Mol Pharm. 2009;6:1631-43.

14. Benet LZ. The role of BCS (biopharmaceutics classification system) and BDDCS (biopharmaceutics drug disposition classification system) in drug development. J Pharm Sci. 2013;102:34-42.

15. Wu CY, Benet LZ. Predicting drug disposition via application of BCS: transport/absorption/ elimination interplay and development of a biopharmaceutics drug disposition classification system. Pharm Res. 2005;22:11-23.

16. Krause DS, Van Etten RA. Tyrosine kinases as targets for cancer therapy. N Engl J Med. 2005;353:172-87.

17. van Erp NP, Gelderblom H, Guchelaar HJ. Clinical pharmacokinetics of tyrosine kinase inhibitors. Cancer Treat Rev. 2009;35:692-706.

18. Di Gion P, Kanefendt F, Lindauer A, Scheffler M, Doroshyenko O, Fuhr U, et al. Clinical pharmacokinetics of tyrosine kinase inhibitors: focus on pyrimidines, pyridines and pyrroles. Clin Pharmacokinet. 2011;50:551-603.

19. Thomas-Schoemann A, Blanchet B, Bardin C, Noe G, Boudou-Rouquette P, Vidal M, et al. Drug interactions with solid tumour-targeted therapies. Crit Rev Oncol Hematol. 2014;89:179-96.

20. de Souza J, Benet LZ, Huang Y, Storpirtis S. Comparison of bidirectional lamivudine and zidovudine transport using MDCK, MDCK-MDR1, and Caco-2 cell monolayers. J Pharm Sci. 2009;98:4413-9.

21. Minematsu T, Giacomini KM. Interactions of tyrosine kinase inhibitors with organic cation transporters and multidrug and toxic compound extrusion proteins. Mol Cancer Ther. 2011;10:531-9.

22. BD Biosciences, BD Gentest™ Pre-Coated PAMPA Plate System: Guidelines for Use.

23. Putnam WS, Pan L, Tsutsui K, Takahashi L, Benet LZ. Comparison of bidirectional cephalexin transport across MDCK and caco-2 cell monolayers: interactions with peptide transporters. Pharm Res. 2002;19:27-33.

24. US Food and Drug Administration, Center for Drug Evaluation and Research. Guidance for Industry - Waiver of in vitro bioavailability and bioequivalence studies for immediate-release solid oral dosage forms based on a Biopharmacetics Classification System. 2000.

25. US Food and Drug Administration. Dasatinib (Sprycel) Summary Basis of Approval. 2006.

26. US Food and Drug Administration. Bosutinib (Bosulif) Summary Basis of Approval. 2012.

27. US Food and Drug Administration. Vandetanib (Caprelsa) Summary Basis of Approval. 2011.

28. Larregieu CA, Benet LZ. Distinguishing between the permeability relationships with absorption and metabolism to improve BCS and BDDCS predictions in early drug discovery. Mol Pharm. 2014;11:1335-44.

29. US Food and Drug Administration. Labetalol HCl Prescribing Information. 2013.

30. Chen ML, Amidon GL, Benet LZ, Lennernas H, Yu LX. The BCS, BDDCS, and regulatory guidances. Pharm Res. 2011;28:1774-8.

31. Chen ML, Yu L. The use of drug metabolism for prediction of intestinal permeability (dagger). Mol Pharm. 2009;6:74-81.

32. Yang Y, Faustino PJ, Volpe DA, Ellison CD, Lyon RC, Yu LX. Biopharmaceutics classification of selected beta-blockers: solubility and permeability class membership. Mol Pharm. 2007;4:608-14.

33. Kusuhara H, Sugiyama Y. In vitro-in vivo extrapolation of transporter-mediated clearance in the liver and kidney. Drug Metab Pharmacokinet. 2009;24:37-52.

34. Lau YY, Huang Y, Frassetto L, Benet LZ. Effect of OATP1B transporter inhibition on the pharmacokinetics of atorvastatin in healthy volunteers. Clin Pharmacol Ther. 2007;81:194-204.

35. Niemi M, Pasanen MK, Neuvonen PJ. Organic anion transporting polypeptide 1B1: a genetically polymorphic transporter of major importance for hepatic drug uptake. Pharmacol Rev. 2011;63:157-81.

36. Shu Y, Brown C, Castro RA, Shi RJ, Lin ET, Owen RP, et al. Effect of genetic variation in the organic cation transporter 1, OCT1, on metformin pharmacokinetics. Clin Pharmacol Ther. 2008;83:273-80.

37. Shu Y, Sheardown SA, Brown C, Owen RP, Zhang S, Castro RA, et al. Effect of genetic variation in the organic cation transporter 1 (OCT1) on metformin action. J Clin Invest. 2007;117:1422-31.

38. Hu S, Chen Z, Franke R, Orwick S, Zhao M, Rudek MA, et al. Interaction of the multikinase inhibitors sorafenib and sunitinib with solute carriers and ATP-binding cassette transporters. Clin Cancer Res. 2009;15:6062-9.

CHAPTER 5. CONCLUSIONS

The discovery of the Philadelphia chromosome and the role of BCR-ABL in the progression of chronic myeloid leukemia have transformed the way that cancers are targeted and treated, and served as the basis for the discovery of other druggable, molecular drivers of various types of cancers. This has led to the development of small molecule tyrosine kinase inhibitors (TKIs) that inhibit the propagation of cell growth and proliferation signals in cancer cells by competing with ATP for binding in the catalytic domain (1). However, as the pharmacologic activity of these drugs is driven by systemic concentrations in the body, factors affecting the pharmacokinetics of TKIs can negatively impact their clinical utility either through the risk of subtherapeutic exposures or drug toxicity. Thus, it was the goal of this work to evaluate the impact of gastric pH and hepatic uptake transporters on TKI drug disposition.

As described in Chapters 2 and 3, many small molecule TKIs are weakly basic drugs and have pH-dependent solubility. These physicochemical characteristics put them at risk for drug-drug interactions with acid-reducing agents (ARAs), such as proton pump inhibitors (PPIs) or H_2-receptor antagonists (H2RAs), due to the elevated gastric pH associated with chronic administration of ARAs resulting in decreased TKI solubility and drug exposure (2). In Chapter 2, we first evaluated the ability of betaine hydrochloride (BHCl), a natural supplement used as a digestive aid, to reacidify gastric pH in healthy volunteers with rabeprazole-induced hypochlorhydria. As expected, the mean fasting gastric pH increased to above pH 5 following multiple doses of rabeprazole (20 mg orally, twice daily), and was significantly decreased after the BHCl administration (1500 mg orally). Furthermore, we demonstrated that the time course

of gastric reacidification was favorable, with a rapid onset of reacidification and sufficient duration to allow for the dissolution of a potential victim drug.

The use of BHCl administration as a potential mitigation strategy for small, molecularly targeted anti-cancer agents was then explored in Chapter 3, using dasatinib as a model compound. Dasatinib is a BCR-ABL TKI used for the treatment of Philadelphia chromosome positive chronic myeloid leukemia or acute lymphoblastic leukemia, and has been shown in previous studies to have significantly reduced maximum plasma concentrations (C_{max}) and drug exposures (area under the concentration-time curve, AUC) when co-administered with famotidine, an H2RA (3). In a three-period crossover study in healthy volunteers, we demonstrated that dasatinib C_{max} and $AUC_{0-\infty}$ were significantly reduced by 94% and 83%, respectively, following concomitant rabeprazole dosing. We also demonstrated that following the addition of 1500mg BHCl after rabeprazole pretreatment, dasatinib C_{max} and $AUC_{0-\infty}$ were significantly increased by 15- and 6.7-fold, respectively, relative to dasatinib with rabeprazole alone. Thus co-administration of BHCl with dasatinib after rabeprazole pretreatment restored dasatinib C_{max} and $AUC_{0-\infty}$ to 90% and 116%, respectively, of the control treatment (dasatinib alone) values. We therefore concluded that the co-administration of BHCl can be an effective mitigation strategy for small, molecularly targeted anti-cancer agents that are weakly basic with pH-dependent solubility between pH 1–4 and that are frequently given with ARAs.

In addition to the impact of gastric pH on dasatinib absorption, we also evaluated the role of hepatic uptake transporters on the drug disposition of small molecule TKIs using the Biopharmaceutics Drug Disposition Classification System (BDDCS), which can predict potentially clinically significant transporter-mediated drug-drug interactions (4). Inhibition of hepatic uptake transporters can result in an increase in drug exposure due to reductions in hepatic

clearance mechanisms in situations where uptake is rate-limiting (5, 6). These interactions can be clinically significant for drugs that are extensively metabolized in the liver, such as TKIs, as increases in drug exposures may increase the risk of unwanted toxicities in patients.

In Chapter 4, we first evaluated the passive permeability rates of dasatinib, bosutinib, and vandetanib *in vitro* using the Parallel Artificial Membrane Permeability Assay (PAMPA) and Caco-2 cell monolayers to experimentally determine BDDCS classification. In comparison to the high permeability rate drug labetalol, all three TKIs had significantly higher passive permeability rates in PAMPA at each concentration and pH tested. We also observed a significant pH effect in the passive permeability rates, with each drug exhibiting a higher passive permeability rate at pH 7.4 versus pH 6.0 due to the basicity of each drug and the higher proportion of nonionzied species at a higher pH. Interestingly however, the opposite trends in A→B permeability rates (relative to labetalol) were observed in Caco-2 cell monolayers. We demonstrated that the inhibition of the efflux transporters P-glycoprotein (P-gp) and Breast Cancer Resistant Protein (BCRP) had no effect on Caco-2 permeability rate, indicating that efflux out of the cells and into the apical chambers could not explain the trend differences between PAMPA and Caco-2 assays. We therefore hypothesize that perhaps the differences between the two assays can be explained by potential effects of protein binding on permeability rate, although this point warrants further investigation.

The difference in results between the two permeability measures however, served as a reminder of the potential limitations of the use of Caco-2 for the prediction of the extent of absorption for classification by the Biopharmaceutics Classification System (BCS), which is highly relevant in drug development for the purposes of biowaivers for highly soluble, extensively absorbed drugs with rapid dissolution (7). Although high permeability rates are

correlated with a high extent of absorption, there are a number of cases in which drugs with poor permeability rates are extensively absorbed (4). Thus, the use of Caco-2 monolayers to predict the extent of absorption may lead to an incorrect BCS classification for drugs that are either hydrophilic or have poor lipophilicity, or drugs permeate the intestinal wall via carrier-mediated or paracellular transport (8).

As our laboratory has previously demonstrated a strong, positive correlation between passive permeability rate and extent of metabolism (4), the high permeability rates of dasatinib, bosutinib, and vandetanib in conjunction with their low solubility (as determined by BCS) classifies them as BDDCS class II compounds, and as such, are potentially affected by efflux transporters in the gut, or uptake and/or efflux transporters in the liver. However, using transfected HEK-293 cell lines and cryopreserved human hepatocytes, we demonstrated that hepatic uptake is not dependent on OCT1 or members of the OATP family (-1B1, -1B3, -2B1), suggesting that passive diffusion is the major route for hepatic transport.

Collectively, the results presented herein demonstrate that for small molecule, weakly basic TKIs with pH-dependent solubility, gastric pH can have a major impact on drug absorption, causing significant reductions in oral bioavailability and systemic exposures of TKIs. These results hold significant clinical relevance as approximately 33% of cancer patients prescribed an anticancer-agent are also prescribed ARAs to manage gastrointestinal disorders (9). However, the magnitude of this interaction may be highly drug dependent as the range in which the solubility is pH-dependent must be considered. We also conclude that co-administration of BHCl can be a potential mitigation strategy for this gastric pH interaction, although the tolerance of BHCl in cancer patients utilizing ARAs to manage gastrointestinal disorders remains a point of consideration.

Unlike gastric pH however, the involvement of hepatic uptake transporters in the transport of dasatinib, bosutinib, and vandetanib was shown to be negligible and drug-drug interactions inhibiting OCT1 or OATPs are not likely to cause significant changes in hepatic clearance. Although the uptake of these TKIs is not mediated via OCT1 or OATPs in the liver, TKI interactions with drug transporters are still important as TKIs can potentially initiate drug-drug interactions for other co-administered drugs dependent on transporters for uptake or efflux.

The results of this work aim to aid in the development of future small molecule TKIs by highlighting potential processes in drug disposition that are of significant importance to TKI pharmacokinetics. In doing so, we hope this translates to the development of more successful TKIs to better treat oncology patients who can benefit from targeted therapies.

REFERENCES

1. Krause DS, Van Etten RA. Tyrosine kinases as targets for cancer therapy. N Engl J Med. 2005;353:172-87.
2. Budha NR, Frymoyer A, Smelick GS, Jin JY, Yago MR, Dresser MJ, et al. Drug absorption interactions between oral targeted anticancer agents and PPIs: is pH-dependent solubility the Achilles heel of targeted therapy? Clin Pharmacol Ther. 2012;92:203-13.
3. Eley T, Luo FR, Agrawal S, Sanil A, Manning J, Li T, et al. Phase I study of the effect of gastric acid pH modulators on the bioavailability of oral dasatinib in healthy subjects. J Clin Pharmacol. 2009;49:700-9.
4. Benet LZ. The role of BCS (biopharmaceutics classification system) and BDDCS (biopharmaceutics drug disposition classification system) in drug development. J Pharm Sci. 2013;102:34-42.
5. Benet LZ. The drug transporter-metabolism alliance: uncovering and defining the interplay. Mol Pharm. 2009;6:1631-43.
6. Kusuhara H, Sugiyama Y. In vitro-in vivo extrapolation of transporter-mediated clearance in the liver and kidney. Drug Metab Pharmacokinet. 2009;24:37-52.
7. US Food and Drug Administration, Center for Drug Evaluation and Research. Guidance for Industry - Waiver of in vitro bioavailability and bioequivalence studies for immediate-release solid oral dosage forms based on a Biopharmacetics Classification System. 2000.

8. Yang Y, Faustino PJ, Volpe DA, Ellison CD, Lyon RC, Yu LX. Biopharmaceutics classification of selected beta-blockers: solubility and permeability class membership. Mol Pharm. 2007;4:608-14.

9. Smelick GS, Heffron TP, Chu L, Dean B, West DA, Duvall SL, et al. Prevalence of acid-reducing agents (ARA) in cancer populations and ARA drug-drug interaction potential for molecular targeted agents in clinical development. Mol Pharm. 2013;10:4055-62.

Publishing Agreement

It is the policy of the University to encourage the distribution of all theses, dissertations, and manuscripts. Copies of all UCSF theses, dissertations, and manuscripts will be routed to the library via the Graduate Division. The library will make all theses, dissertations, and manuscripts accessible to the public and will preserve these to the best of their abilities, in perpetuity.

Please sign the following statement:

I hereby grant permission to the Graduate Division of the University of California, San Francisco to release copies of my thesis, dissertation, or manuscript to the Campus Library to provide access and preservation, in whole or in part, in perpetuity.

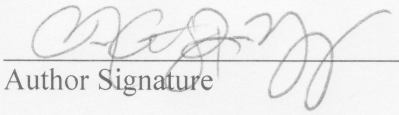

Author Signature

03/25/2015

Date